Report No. CG-D-13-94

AD-A282 650

The Effects Of Aspect Ratio, Section Shape, And Reynolds Number On The Lift And Drag Of A Series Of Model Control Surfaces

Edward M. Lewandowski

Davidson Laboratory
Stevens Institute of Technology
Castle Point Station
Hoboken, NJ 07030

FINAL REPORT
JUNE 1994

This document is available to the U.S. public through the National Technical Information Service, Springfield, Virginia 22161

Prepared for:

U.S. Coast Guard
Research and Development Center
1082 Shennecossett Road
Groton, CT 06340-6096

and

U.S. Department of Transportation
United States Coast Guard
Office of Engineering, Logistics, and Development
Washington, DC 20593-0001

NOTICE

This document is disseminated under the sponsorship of the Department of Transportation in the interest of information exchange. The United States Government assumes no liability for its contents or use thereof.

The United States Government does not endorse products or manufacturers. Trade or manufacturers' names appear herein solely because they are considered essential to the object of this report.

The contents of this report reflect the views of the Coast Guard Research & Development Center. This report does not constitute a standard, specification, or regulation.

D. L. Motherway
Technical Director, Acting
United States Coast Guard
Research & Development Center
1082 Shennecossett Road
Groton, CT 06340-6096

Technical Report Documentation Page

1. Report No.	2. Government Accession No.	3. Recipient's Catalog No.
CG-D-13-94		

4. Title and Subtitle

The Effects of Aspect Ratio, Section Shape, and Reynolds Number on the Lift and Drag of a Series of Model Control Surfaces

5. Report Date June 1994

6. Performing Organization Code

7. Author(s) Edward M. Lewandowski

8. Performing Organization Report No. R&DC 06/91

9. Performing Organization Name and Address

Davidson Laboratory
Stevens Institute
Castle Point Station
Hoboken, NJ 07030

10. Work Unit No. (TRAIS)

11. Contract or Grant No. N00014-84-C-0644

12. Sponsoring Agency Name and Address

U.S. Coast Guard
Research and Development Center
1082 Shennecossett Road
Groton, Connecticut 06340-6096

Department of Transportation
U.S. Coast Guard
Office of Engineering, Logistics, and Development
Washington, D.C. 20593-0001

13. Type of Report and Period Covered Final Report

14. Sponsoring Agency Code

15. Supplementary Notes

16. Abstract

The report presents the results of towing tank tests on a series of fins, representative of the canards on a SWATH vessel or the rudders on a planing hull. The work was done to determine whether or not the fins and rudders on a small model suffered from serious scale effects.

Fins with aspect ratios of 1.0, 1.5 and 2.0 were mounted vertically under a horizontal flat plate and towed at a series of speeds resulting in five Reynolds numbers, based on chord length, between 42,000 and 150,000. The fins had both flat plate and NACA 0015 cross sections, and were tested with and without turbulence trips. Lift and drag forces were measured at a series of angles of attack which were varied from 0 to 35 degrees in five degree increments. The measured lift slopes agreed well with predictive equations developed at DTNSRDC for fins at high Reynolds numbers. This means that dynamic stability and course keeping data taken using small models can be used in making full scale predictions.

17. Key Words

control surfaces
fins
SWATH control
aspect ratio effects
Reynolds number effects
turbulence trips
rudders

18. Distribution Statement

Document is available to the U.S. public through the National Technical Information Service, Springfield, Virginia 22161

19. Security Classif. (of this report)	20. SECURITY CLASSIF. (of this page)	21. No. of Pages	22. Price
UNCLASSIFIED	UNCLASSIFIED		

Form DOT F 1700.7 (8/72) Reproduction of form and completed page is authorized

METRIC CONVERSION FACTORS

Approximate Conversions to Metric Measures

Symbol	When You Know	Multiply By	To Find	Symbol
		LENGTH		
in	inches	*2.5	centimeters	cm
ft	feet	30	centimeters	cm
yd	yards	0.9	meters	m
mi	miles	1.6	kilometers	km
		AREA		
in^2	square inches	6.5	square centimeters	cm^2
ft^2	square feet	0.09	square meters	m^2
yd^2	square yards	0.8	square meters	m^2
mi^2	square miles	2.6	square kilometers	km^2
	acres	0.4	hectares	ha
		MASS (WEIGHT)		
oz	ounces	28	grams	g
lb	pounds	0.45	kilograms	kg
	short tons (2000 lb)	0.9	tonnes	t
		VOLUME		
tsp	teaspoons	5	milliliters	ml
tbsp	tablespoons	15	milliliters	ml
fl oz	fluid ounces	30	milliliters	ml
c	cups	0.24	liters	l
pt	pints	0.47	liters	l
qt	quarts	0.95	liters	l
gal	gallons	3.8	liters	l
ft^3	cubic feet	0.03	cubic meters	m^3
yd^3	cubic yards	0.76	cubic meters	m^3
		TEMPERATURE (EXACT)		
°F	Fahrenheit temperature	5/9 (after subtracting 32)	Celsius temperature	°C

*1 in = 2.54 (exactly).

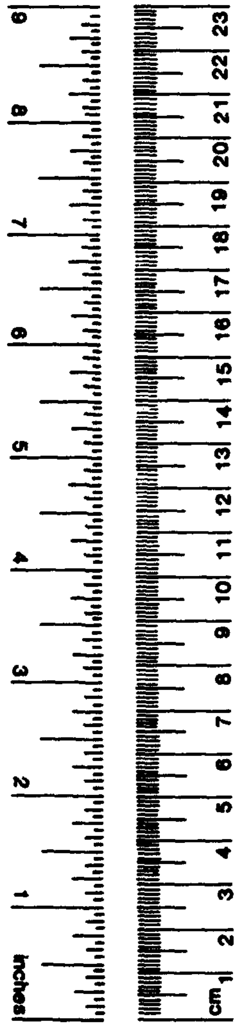

Approximate Conversions from Metric Measures

Symbol	When You Know	Multiply By	To Find	Symbol
		LENGTH		
mm	millimeters	0.04	inches	in
cm	centimeters	0.4	inches	in
m	meters	3.3	feet	ft
m	meters	1.1	yards	yd
km	kilometers	0.6	miles	mi
		AREA		
cm^2	square centimeters	0.16	square inches	in^2
m^2	square meters	1.2	square yards	yd^2
km^2	square kilometers	0.4	square miles	mi^2
ha	hectares (10,000 m^2)	2.5	acres	
		MASS (WEIGHT)		
g	grams	0.035	ounces	oz
kg	kilograms	2.2	pounds	lb
t	tonnes (1000 kg)	1.1	short tons	
		VOLUME		
ml	milliliters	0.03	fluid ounces	fl oz
l	liters	0.125	cups	c
l	liters	2.1	pints	pt
l	liters	1.06	quarts	qt
l	liters	0.26	gallons	gal
m^3	cubic meters	35	cubic feet	ft^3
m^3	cubic meters	1.3	cubic yards	yd^3
		TEMPERATURE (EXACT)		
°C	Celsius temperature	9/5 (then add 32)	Fahrenheit temperature	°F

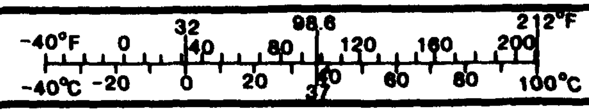

TABLE OF CONTENTS

ABSTRACT

A series of fins, representing the canards of a SWATH vessel, were tested on a groundboard in a towing tank. Fins having three aspect ratios, with flat plate and NACA 0015 sections, were tested with and without turbulence trips. Lift and drag of the fins were measured at angles of attack from 0° to 35° over a range of Reynolds numbers from 42,000 to 150,000. Measured lift curve slopes agree well with predictions and the results of previous high Reynolds number tests.

KEYWORDS

Control surfaces
Fins
SWATH control
Aspect ratio
Reynolds number
Turbulence trips
Rudders

LIST OF TABLES

LIST OF FIGURES

LIST OF FIGURES (Concluded)

NOMENCLATURE

A	Geometric aspect ratio, b^2/S
A_e	Effective aspect ratio, 2A
a_o	Section lift curve slope, per radian
b	Fin span, ft
C	A calibration matrix (See Appendix A)
C_D	Drag coefficient, $D/(1/2\ \rho\ V^2 S)$
C_{Do}	Profile drag coefficient
$C_{D.}$	Drag coefficient based on frontal area
C_L	Lift coefficient, $L/(1/2\ \rho\ V^2 S)$
c	Fin mean chord, S/b, ft
D	Drag, lb
L	Lift, lb
R	A calibration matrix (See Appendix A)
R_{ij}	Element of calibration matrix
Re	Reynolds number, Vc/ν
S	Planform area, ft^2
s	Standard deviation
V	Velocity, ft/sec
V_1	Digitized voltage due to lift
V_2	Digitized voltage due to drag
α	Angle of attack, degrees
ρ	Density of water, $slug/ft^3$
ν	Kinematic viscosity, ft^2/sec

INTRODUCTION

The Davidson Laboratory is supporting the U.S. Coast Guard in a research program directed at improving our understanding of SWATH pitch control, by conducting a series of model tests. The control surfaces on models operate at substantially lower Reynolds numbers than those on a prototype vessel: Control surfaces on a SWATH may be operating at Reynolds numbers of about 6 million, while those on a model may operate at only 200,000 at the corresponding Froude number. In order for the control system to be properly modeled, it is therefore essential that Reynolds number effects be considered. The phase of the study described in this report was directed toward a determination of the effects of Reynolds number, section shape, aspect ratio and turbulence stimulation on the behavior of the control surfaces.

To determine whether scale hydrofoil sections or flat plate sections provide a better simulation of full-scale hydrofoil sections at low Reynolds numbers, tests were conducted on a series of fins mounted on a groundboard and towed over a range of Reynolds numbers likely to be experienced during typical model tests. The fins had geometric aspect ratios of 1.0, 1.5, and 2.0 with both flat plate and NACA 0015 sections. All fins had a planform area of 0.04396 square feet and a taper of 0.454, with zero sweep at the 30% chord line. The fins are representative of the U.S. Coast Guard SWATH 10 vessel[1] [superscripts refer to references on page 11]; the area (for a scale of 1/24) and taper are those of the original design, and the original aspect ratio of 1.1945 is bracketed by the series.

Lift and drag of the fins were measured, for angles of attack of 0° to 35°, over a speed range chosen to include the "critical Reynolds numbers" at which Schmitz[2] found a jump in the lift coefficient in wind tunnel tests of airfoil sections.

Again with the aim of providing the best simulation of full-scale hydrofoil sections, the effect of turbulence trips on lift and drag was also investigated: Each fin was tested with and without Hama strips3.

Tests were conducted in the Davidson Laboratory Tank 3 facility in March, 1987.

DESCRIPTION OF MODELS

Plan and section views of the three fins are shown on Figure 1, which gives all important dimensions. The fins all have a planform area, S, of 0.04396 square feet, a taper ratio of 0.454, and 0 degrees sweep at the 30% chord line. The section shape of the flat plate was chosen to be similar to the flat plate section tested by Schmitz (reference 2 plate II).

The flat plate fins were made from 1/8 inch aluminum plate. The NACA 0015 section fins were constructed from plexiglass, with 1/4 inch stainless steel shafts.

Turbulence stimulation was provided by Hama strips. The strips were made from a double thickness of electrical tape 0.25 inch wide, cut with pinking shears to form a serrated leading edge, and attached to the fins as shown on Sketch A below:

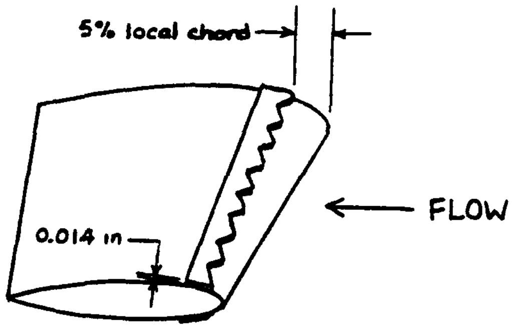

SKETCH A. HAMA STRIPS.

This configuration was found by Hama et al[3] to be "better than any known way of turbulence stimulation", effectively creating the three-dimensional vortex loops within the boundary layer which apparently lead to laminar-to-turbulent breakdown, with minimal parasitic drag.

The critical Reynolds number based on trip thickness and flow velocity at the top of the trip was estimated by Hama et al to be about 45. For these tests the Reynolds number based on trip thickness and model velocity at the lowest test speed was 233. Thus the trips were expected to be fully effective at all test speeds.

The effect of trip thickness was briefly investigated, at zero angle of attack, on the aspect ratio 1 fins. Runs were made with a double and a triple layer Hama strip at the highest Reynolds number, with the aim of evaluating the parasitic drag of the trips.

In addition, some runs were made using a trip wire as the transition device. The diameter (1/32 inch) was selected to satisfy the criterion given by Preston[4] for a fully effective trip.

APPARATUS

The apparatus is shown on Figures 2 (photograph) and 3 (drawing). It consisted of a horizontal plate (the ground board), 10 inches wide, 16 inches long, and 3/16 inch thick, which was towed 1 inch below the water surface. At the center of the plate was a hole through which the shafts of the fins passed to connect to the bottom of the lift and drag balances. The upper end of the shaft was equipped with a pointer for use in setting angles of attack. The pointer was adjusted for each fin so that zero angle of attack corresponded to zero lift. The gap between the plate and the fin was approximately 0.04 inch.

Because some underwater photographs showed that air was being drawn down through the hole in the flat plate on the suction side of the fins in some cases, a seal was constructed using a thin rubber sheet, as shown schematically on Sketch B below:

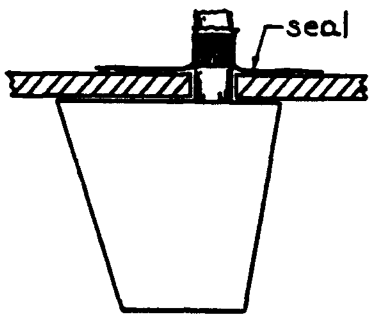

SKETCH B. THIN RUBBER SEAL.

Subsequent underwater photographs, such as Figure 4 ($\alpha=25^{\circ}$, V=7.34 fps) showed that the seal was effective. Because the edges of the seal were not fastened down, no effect on the calibration rates was expected.

Figure 5 is a running photograph of the apparatus, showing the method of attachment to the towing carriage (the heave masts visible in the photograph were clamped; the apparatus was not free to heave). The photograph shows the inclinometer (attached to the uppermost plate, aft of the vertical posts). The running trim of the apparatus was monitored during the tests, to ensure that the horizontal plate maintained a very slight bow up attitude (typically 0.2 degree) so that the flow over the bottom of the plate would not separate at the leading edge.

TEST PROGRAM

The six fins were tested over a range of Reynolds numbers and angles of attack, with and without turbulence stimulation, as summarized in Table A below. Reynolds numbers are based on mean chord length.

TABLE A. TEST MATRIX.

Geometric aspect ratio	1, 1.5, 2
Section shape	Flat plate, NACA 0015
Turbulence stimulation	With and without
Reynolds number	42,000, 75,000, 100,000, 125,000, 150,000
Angle of attack, degrees	0, 5, 10, 15, 20, 25, 30, 35

In addition to this basic matrix, additional runs were made at intermediate angles of attack in the vicinity of the stall angle.

TEST PROCEDURE

Calibration

The balance was calibrated by applying known weights in the directions of lift, drag, and combinations of the two, taking voltage readings on both channels, and using a multivariate least squares fit to express the digitized voltage readings as linear functions of both lift and drag. The resulting matrix of coefficients was next inverted to obtain the calibration rates. The procedure is explained in detail in Appendix A, which includes calibration results, plots, and a photograph of the calibration setup. The calibration was checked daily.

The balance was found to undergo small angular deflections under load. To evaluate the resulting change in angle of attack, deflection was calibrated against lift. Details are given in Appendix A.

Procedure

After setting the fin to the desired angle of attack, zero readings were taken on the lift and drag channels. Running readings were taken in a 50 foot run length after steady speed had been achieved. The averaged running readings, minus the zero readings, were then multiplied by the calibration rates to obtain measured lift and drag. After covering the speed range at a set angle of attack, the next angle was set and new zero readings were taken.

To help quantify the precision of the measurements, repeat runs (including angle resets) were made at several conditions.

Early in the test program, it was suspected that under some conditions, air was being drawn down through the hole in the ground board on the suction side of the fins, reducing the lift. Underwater cameras were set up to check this; the photographs showed that ventilation was indeed taking place. The thin rubber seal described in the Apparatus section was then installed. Underwater photographs were then taken during 15 subsequent runs at conditions under which ventilation had either been observed or suspected. No ventilation was observed in these photographs. Polaroid shots were taken periodically throughout the remainder of the test program to ensure that no ventilation was taking place.

The running trim of the apparatus was monitored as discussed in the Apparatus section, and all signals were monitored on a tankside oscillograph chart recorder. The tank water temperature was recorded daily. A tabulation of temperature readings appears in Appendix B.

RESULTS

Test data are tabulated in Tables 2-7, which list run number, towing speed in fps, the set and corrected angle of attack (see Apparatus and Appendix A), measured lift and drag in pounds, and lift and drag coefficients. Table 1 is a brief directory of the data tables.

The data are presented in the form of carpet plots on Figures 6-19. Such a presentation shows the behavior of the dependent variable (C_L or C_D) with the two independent variables (angle of attack and Reynolds number), and permits fairing of curves through the data simultaneously in three dimensions. The departure of the curves of constant α from the horizontal in these figures is an indication of the degree of the dependence of the coefficients on Reynolds number. It should be noted that the lift curves (Figures 6-17) show the behavior only up to the apparent stall angle; the curves at higher angles of attack bend over and thus would fall "behind" the carpet.

As an example of the interpretation of the carpet plots, it is supposed that the lift coefficient of the aspect ratio 1 NACA 0015 fin without turbulence trips is required, at $\alpha=10^{\circ}$ and Re=100,000. Referring to Figure 12, the point of intersection of the $\alpha=10^{\circ}$ contour (horizontal) with the Re=100,000 contour (diagonal) is first located. Then, the value of C_L at this point is read from the vertical scale (draw a line perpendicular to the axis through the point of interest): $C_L=0.39$.

The curves on Figures 20-25 have been taken directly from the carpet plots and are superimposed to facilitate comparison. These figures illustrate the effects of aspect ratio, section shape, and turbulence trips on the lift curves. Figure 26 shows the effect of section shape on drag coefficient.

The behavior of drag coefficient with Reynolds number at $\alpha=0^{\circ}$ is shown on Figure 27. The effect of turbulence trips is also shown.

The results for the NACA 0015 fins are presented in the form of drag polars on Figure 28; Figure 29 shows the effect of section shape on the drag polar.

The effect of Hama strips and trip wires on the behavior of lift coefficient with Reynolds number is illustrated on Figure 30.

Precision

At least five repeat runs were made at the following conditions:

a) Flat plate section, A=1, $\alpha=10^{\circ}$, Re=150,000, n=5
b) Flat plate section, A=1.5, $\alpha=20^{\circ}$, Re=150,000, n=7
c) NACA 0015 section, A=1, $\alpha=10^{\circ}$, Re=150,000, n=9

(13 runs were actually performed at the second condition, but only 7 of these involved resetting the angle). The statistics

for these repeat runs are presented in Table B below. Based on these repeat runs, using the method of Reference 5, the precision of the data may be quantified as follows: The probability is 0.95 that at least 80% of the lift measurements will be within ±0.14 lb. The probability is 0.95 that at least 80% of the drag measurements will be within ±0.03 lb.

TABLE B. STATISTICS OF REPEAT RUNS.

Group	Mean Lift lb	s lb	s/Mean
a)	1.026	0.028	0.027
b)	2.559	0.116	0.045
c)	0.927	0.014	0.015

Group	Mean Drag lb	s lb	s/Mean
a)	0.198	0.019	0.097
b)	1.051	0.015	0.014
c)	0.140	0.000	0.000

The lift data in the second group of repeats ($\alpha=20^{\circ}$) has more scatter than the other two groups. Figure 6 shows that $\alpha=20^{\circ}$ is very near stall for this fin so that unsteadiness associated with separation may account fc some of this scatter. If the second group is not considered in the analysis, the precision statement becomes: The probability is 0.95 that at least 70% of the lift measurements are within %0.03 lb, for angles of attack below stalling. The probability is 0.95 that at least 70% of the lift measurements will be within ±0.03 lb, for angles of attack below stalling.

DISCUSSION

Reynolds Number Effects

Reference to Figures 6-17 shows that the effect of Reynolds number on the lift coefficient is small for all of the fins tested. This is evidenced by the fact that the lines of constant angle of attack in the figures are nearly horizontal. In particular, no jump in the lift coefficient in the range of Reynolds numbers of 60,000-80,000, where Schmitz[2] found a discontinuity, was observed. However it should be noted that with the exception of the flat plate, all of the sections tested by Schmitz had camber; examination of his data shows that the jump seems to be due to a shift in the angle of zero lift with Reynolds number. For his N60 section, which most closely resembles the NACA 0015 section tested here, the lift curves are essentially parallel in the range of Reynolds numbers between 21,000 and 8 million.

Whicker and Fehlner[6] tested a series of control surfaces in a wind tunnel, two of which had the same aspect ratio, taper, and section shape (NACA 0015) as two of the fins tested in the present study. The Reynolds number range of the Whicker-Fehlner tests was approximately 1 to 3 million. A comparison of their results with those of the present study is given on Figure 31. Aside from the expected effect of Reynolds number on maximum lift coefficient, the agreement is quite good. Thus it may be expected that, below the stall angle, small scale appendages will correctly model the full scale lift.

Comparison of the flat plate data with the NACA section data shows that the lift of the flat plate sections is generally more sensitive to Reynolds number than that of the NACA sections.

Reynolds number effects on drag are illustrated on Figures 18 and 19 for the aspect ratio 2 NACA fin with and without [illegible]a strips, respectively. In Figure 18 the constant angle of a[illegible]k contours have a steeper slope than the Schoenherr line (see [illegible]so Figure 27). This is due to the characteristic behavior of airfoils at low Reynolds numbers when the form drag is relatively large[7]. With turbulence trips, the lines of constant a become more parallel to the Schoenherr line and are shifted upwards. The jump in the curves near $\alpha=10^{\circ}$ is associated with stall.

Aspect Ratio

The effect of aspect ratio on lift coefficient for the flat plates and NACA 0015 fins is shown on Figures 20 and 21. As expected, the lift curves become steeper with increasing aspect ratio. For the NACA section, C_{Lmax} is unaffected by aspect ratio; C_{Lmax} decreases with increasing aspect ratio for the flat plate fins.

The lift curve slope at the origin was obtained by using the slope of the faired carpet plot curves between $\alpha=0^{\circ}$ and $\alpha=5^{\circ}$. Results for the NACA 0015 fins without trips at Re=150,000 are summarized in Table C below.

TABLE C. LIFT CURVE SLOPE.

A	Slope (per degree)	Theory
1.0	0.040	0.041
1.5	0.048	0.051
2.0	0.060	0.058

Theoretical results were obtained by use of the formula

$$dC_L/d\alpha = a_o/(1 + 1/A_e + a_o/\pi A_e) \quad (1)$$

which is the result of finite aspect ratio wing theory including the Jones edge correction factor[8]. The effective aspect ratio A_e was taken to be 2A, as is generally done for fins on a groundboard. The section lift curve slope, a_o, is given by Whicker and Fehlner[6] "corrected from experimental observations":

$$a_o = (0.9)2\pi$$

Hence the lift coefficient may be expressed as

$$C_L = 1.8\pi\alpha/(1 + 2.8/A_e) \quad (2)$$

Agreement with this semi-empirical relationship is quite good.

The effect of aspect ratio on drag is illustrated by the drag polars on Figure 28. Induced drag apparently decreases with increasing aspect ratio, as expected. The drag of a finite wing (without camber or twist) can in theory be expressed as

$$C_D = C_{Do} + KC_L^2/\pi A_e \quad (3)$$

where C_{Do} is the profile drag coefficient and K is the induced drag factor. Figure 32 was prepared to determine the factor K, for NACA sections without Hama strips. This figure shows the apparent induced drag coefficient, $C_D - C_{Do}$, against the ratio C_L^2/A_e where as before $A_e = 2A$ to account for the groundboard (the profile drag was assumed to correspond to the drag at zero lift). The least-squares linear fit shown on the figure, together with Equation (3), indicate that $K/\pi = 0.7321$, or $K = 2.30$.

Section Shape

The effect of section shape on the lift curve slope is shown on Figures 22 and 23. The flat plate lift is generally higher than the NACA section lift, and the behavior without trips is less linear (also compare Figures 6, 8, 10 to 12, 14, 16). In general C_{Lmax} is larger for the flat plate fins in the range of Reynolds numbers examined.

Figure 26 shows the effect of section shape on drag. For angles of attack above 0^o and below 25^o, the drag of the flat plate is larger; this is probably due to the presence of the sharp angle at the end of the tapered nose of the section (Figure 1).

The effect of the section shape on the apparent induced drag is shown on Figure 29. The drag polars are virtually coincident up to stall.

Turbulence Trips

The results of Schmitz[2] and several studies cited by Goldstein[7] indicate that in most cases turbulent flow is beneficial to the lift of airfoils. In his section on "notes for teaching the physics of flight", Schmitz describes an experiment in which placing a turbulence grid in front of a round nosed, thick profile resulted in "two to three times the lift value, according to the angle of incidence". Goldstein shows that C_{Lmax} increases in general with turbulence of the stream. However, surface roughness is known to degrade the performance of full scale airfoils[7,8]. An attempt was made in the present study to determine which of these effects is dominant for model appendages.

The effect of the trips (Hama strips) on lift is highlighted in Figures 24 and 25 for the flat plate and NACA sections, respectively. The trips generally decrease the lift coefficient but for the NACA section increase C_{Lmax}. The trips also tend to make the lift curves more linear.

Figure 24 indicates that the detrimental effect of the Hama strips on the flat plate lift is substantial. To determine whether another tripping device would produce better results, a series of tests was made with the aspect ratio 1.5 flat plate using trip wires (as described above under Model). The results are presented on Figure 30 as curves of C_L at constant angle of attack against Reynolds number. The curves show a very slight increase in lift with Reynolds number for the untripped fin, but a noticeable drop when the Hama strip is used; the reduction of lift due to the trip wire was greater still. It would appear that on the flat plate the trips promote separation.

Comparison of Figures 18 and 19 shows that the trips have two salient effects on drag coefficient: a shift of the curves of C_D at constant α upwards, and an upward shift of the jump in the curves of constant Re (occurring near α=15o). The former shift is presumably due to a combination of turbulent flow and parasitic drag of the trip. The jump is associated with stall, and since the tripped foil stalls at a higher angle of attack (17.5° vs 13.5°) the drag jump would be expected to occur at a higher angle also.

Figure 27 shows the behavior of the drag coefficient of an NACA section fin at zero angle of attack with Reynolds number. The data for the untripped fin show a definite downward trend relative to the Schoenherr line whereas the data for the tripped fin lie practically parallel to the Schoenherr line. This would support the hypothesis that the trips are effective in producing a turbulent boundary layer.

In an attempt to evaluate the parasitic drag of the Hama strips, runs were made with a double and a triple thickness (four and six layers of electrical tape) on the aspect ratio 1 fins at zero angle of attack. Results are shown on Figure 33. C_D is linear with trip thickness, and corresponds to a drag coefficient based on the frontal area of the trips of

$$C_{D.} = 1.25 \tag{4}$$

CONCLUSIONS

Based on the results of this experimental study and the discussion above, the following conclusions may be drawn:

1. Lift coefficients of the fins are not strongly affected by variations of the Reynolds number in the range covered by the tests (42,000 - 150,000). The NACA 0015 fins are less sensitive to Reynolds number than the flat plate sections; C_L results of this study for NACA 0015 fins are in agreement with previous experimental data[6] obtained at Reynolds numbers of 1 million and higher.

2. Lift coefficients of the flat plate sections are generally higher at the same angle of attack than NACA 0015 fins of the same planform. The lift curves of the untripped flat plates are more nonlinear than those of the NACA sections.

3. When placed on the flat plate fins, turbulence trips reduce the lift coefficient by an amount which increases with Reynolds number. The trips cause a small reduction of the lift curve slope of the NACA section fins but cause an increase in the maximum lift coefficient.

4. Hama strips seem to be effective in inducing a turbulent boundary layer on the NACA 0015 fins in the Reynolds number range of the tests.

5. Drag coefficients of the flat plate fins are generally higher than those of the NACA 0015 fins, possibly due to separation at the end of the nose taper (see Figure 1).

RECOMMENDATIONS

The aim of this study was to determine whether hydrofoil sections or flat plate sections provide a better simulation of full-scale hydrofoil sections at low Reynolds numbers. The results have shown that the scale hydrofoil sections are best, as indicated by conclusions 1 and 2. The data of Reference 6, taken at Reynolds numbers of 1 to 3 million, can be taken to be indicative of full-scale conditions (the Reynolds number of the aspect ratio 1 fin on a SWATH vessel at 10 knots would be about 6.6 million); the lift data of the present study for NACA 0015 fins are in agreement with Reference 6 (apart from the expected reduction in maximum lift coefficient) whereas the flat plate data are generally higher and less linear with angle of attack. Thus it is recommended that scale hydrofoil sections be used for model control surfaces.

The use of Hama strips on the NACA 0015 fins is recommended for the upcoming tests of the SWATH model with pitch control, because of their effect on C_{Lmax}. The effect of a slight reduction of the lift curve slope due to the trips can be compensated for by making the model fins slightly larger than scale area, or by adjustment of control system gains. The larger C_{Lmax} results in a larger available pitch moment for the control of pitching motion.

REFERENCES

1. Klosinski, W.E., and Numata, E., "Powering and Seakeeping Tests of a U.S. Coast Guard SWATH Cutter Design", Davidson Laboratory Report No. 2515, October 1984.

2. Schmitz, F.W., **Aerodynamics of Model Aircraft (Aerodynamik des Flugmodells)**, Carol Lange Verlag, Duisburg, Germany, 1952 (Ministry of Aircraft Production Translation No. 2460).

3. Hama, F.R., Long, J.D., and Hegarty, J.C., "On Transition from Laminar to Turbulent Flow", University of Maryland Technical Note BN-81, August 1956.

4. Preston, J.H., "The Minimum Reynolds Number for a Turbulent Boundary Layer and the Selection of a Transition Device", Journal of Fluid Mechanics, Volume 3, Part 4, January 1958.

5. Brown, P.W., "Assessment of Experimental Precision", Davidson Laboratory Note 563, October 1959.

6. Whicker, L.F., and Fehlner, L.F., "Free-Stream Characteristics of a Family of Low Aspect Ratio, All-Moveable Control Surfaces fpor Application to Ship Design", DTNSRDC Research and Development Report 933, December 1958.

7. Goldstein, S., **Modern Developments in Fluid Dynamics**, Volume II, THe Clarendon Press, Oxford, 1950, Chapter 10.

8. Abbott, I.H., and von Doenhoff, A.E., **Theory of Wing Sections**, Dover Publications, New York, 1959.

9. Glauert, H., **The Elements of Airfoil and Airscrew Theory**, 2nd Ed., University Press, Cambridge, 1959.

TABLE 1

Directory of Data Tables

Table no.	Section shape	Aspect ratio	Hama strip	Figure no.
2a	flat	1.0	no	6
2b	flat	1.0	yes	7
3a	flat	1.5	no	8
3b	flat	1.5	yes	9
3c	flat	1.5	trip wire	30
4a	flat	2.0	no	10
4b	flat	2.0	yes	11
5a	NACA 0015	1.0	no	12,28
5b	NACA 0015	1.0	yes	13
6a	NACA 0015	1.5	no	14,28
6b	NACA 0015	1.5	yes	15
7a	NACA 0015	2.0	no	16,18,28
7b	NACA 0015	2.0	yes	17,19

Table 2a

Flat plate section, aspect ratio 1.

Run no.	Speed fps	α set	α corr.	Lift lb	Drag lb	C_L	C_D
			Re = 42,000				
333	2.05	0.0	0.0	0.01	0.00	0.051	0.016
334	2.05	5.0	5.0	0.05	0.01	0.259	0.039
335	2.05	10.0	10.0	0.10	0.02	0.538	0.131
361	2.05	10.0	10.0	0.09	0.02	0.484	0.093
360	2.05	15.0	15.0	0.11	0.03	0.616	0.192
363	2.04	20.0	20.0	0.14	0.05	0.795	0.300
368	2.05	22.0	22.0	0.15	0.06	0.820	0.342
373	2.04	25.0	25.0	0.15	0.07	0.839	0.402
374	2.04	30.0	30.0	0.12	0.08	0.698	0.435
375	2.04	35.0	35.0	0.12	0.09	0.680	0.519
			Re = 75,000				
84	3.65	-10.0	-10.0	-0.25	0.05	-0.442	0.096
81	3.62	0.0	0.0	-0.01	0.01	-0.019	0.024
49	3.62	5.0	5.0	0.13	0.02	0.228	0.038
57	3.62	10.0	10.0	0.26	0.05	0.463	0.082
67	3.62	10.0	10.0	0.26	0.05	0.460	0.092
62	3.62	15.0	14.9	0.37	0.11	0.657	0.190
68	3.62	20.0	19.9	0.49	0.23	0.877	0.403
364	3.67	20.0	19.9	0.45	0.18	0.792	0.309
369	3.67	22.0	21.9	0.47	0.20	0.827	0.353
387	3.67	22.0	21.9	0.47	0.20	0.814	0.347
89	3.65	25.0	24.9	0.41	0.20	0.725	0.359
93	3.65	30.0	29.9	0.40	0.24	0.711	0.422
97	3.65	35.0	34.9	0.41	0.29	0.720	0.516
			Re = 100,000				
82	4.82	0.0	0.0	0.00	0.02	0.001	0.022
50	4.82	5.0	5.0	0.23	0.04	0.230	0.039
59	4.82	10.0	9.9	0.45	0.09	0.458	0.086
63	4.82	15.0	14.9	0.66	0.18	0.664	0.186
69	4.82	20.0	19.9	0.81	0.38	0.820	0.387
70	4.82	20.0	19.9	0.80	0.38	0.807	0.386
365	4.87	20.0	19.9	0.78	0.30	0.772	0.300
382	4.89	20.0	19.9	0.77	0.30	0.758	0.293
370	4.89	22.0	21.9	0.82	0.35	0.809	0.343
388	4.89	22.0	21.9	0.81	0.34	0.791	0.337
90	4.85	25.0	24.9	0.69	0.34	0.687	0.341
384	4.90	25.0	24.9	0.73	0.38	0.713	0.370
94	4.85	30.0	29.9	0.66	0.40	0.660	0.396
98	4.85	35.0	34.9	0.67	0.49	0.667	0.487

Table 2a (Concluded)

Flat plate section, aspect ratio 1.

Run no.	Speed fps	α set	α corr.	Lift lb	Drag lb	C_L	C_D
			Re = 125,000				
83	6.04	0.0	0.0	-0.01	0.03	-0.009	0.021
51	6.04	5.0	4.9	0.35	0.06	0.228	0.038
60	6.03	10.0	9.9	0.72	0.13	0.463	0.087
64	6.04	15.0	14.8	1.01	0.29	0.649	0.185
71	6.03	20.0	19.8	1.24	0.59	0.801	0.382
366	6.12	20.0	19.8	1.22	0.47	0.763	0.297
371	6.12	22.0	21.8	1.27	0.54	0.795	0.338
389	6.12	22.0	21.8	1.24	0.53	0.776	0.333
91	6.05	25.0	24.8	1.00	0.51	0.644	0.324
95	6.05	30.0	29.8	1.02	0.61	0.653	0.391
99	6.07	35.0	34.8	1.03	0.75	0.654	0.477
			Re = 150,000				
85	7.26	-10.0	-9.8	-1.01	0.22	-0.451	0.097
48	7.23	0.0	0.0	0.02	0.05	0.009	0.022
80	7.24	0.0	0.0	-0.01	0.05	-0.006	0.022
332	7.28	0.0	0.0	0.02	0.04	0.010	0.018
52	7.24	5.0	4.9	0.51	0.08	0.227	0.036
61	7.23	10.0	9.8	1.03	0.19	0.464	0.087
86	7.28	10.0	9.8	0.98	0.17	0.434	0.076
336	7.28	10.0	9.8	1.02	0.20	0.454	0.088
359	7.28	10.0	9.8	1.04	0.21	0.462	0.094
362	7.31	10.0	9.8	1.06	0.22	0.468	0.095
65	7.23	15.0	14.8	1.45	0.41	0.651	0.185
88	7.28	15.0	14.8	1.40	0.39	0.621	0.172
72	7.23	20.0	19.7	1.76	0.82	0.792	0.369
87	7.27	20.0	19.7	1.71	0.62	0.761	0.275
367	7.33	20.0	19.7	1.74	0.68	0.763	0.298
372	7.31	22.0	21.7	1.81	0.76	0.796	0.335
390	7.33	22.0	21.7	1.74	0.74	0.761	0.326
385	7.39	25.0	24.7	1.56	0.82	0.673	0.351
92	7.27	25.0	24.8	1.49	0.72	0.661	0.322
96	7.27	30.0	29.8	1.46	0.87	0.649	0.386
100	7.28	35.0	34.8	1.45	1.07	0.641	0.472

Table 2b

Flat plate section, aspect ratio 1, with Hama strips.

Run no.	Speed fps	α set	α corr.	Lift lb	Drag lb	C_L	C_D
			Re = 42,000				
377	2.04	0.0	0.0	0.01	0.01	0.041	0.036
378	2.04	5.0	5.0	0.04	0.01	0.217	0.050
379	2.04	10.0	10.0	0.07	0.02	0.415	0.090
380	2.04	15.0	15.0	0.11	0.03	0.613	0.182
381	2.04	20.0	20.0	0.13	0.05	0.760	0.287
386	2.05	22.0	22.0	0.14	0.06	0.809	0.337
383	2.04	25.0	25.0	0.12	0.06	0.690	0.364
391	2.05	25.0	25.0	0.13	0.07	0.728	0.371
392	2.05	30.0	30.0	0.11	0.08	0.632	0.422
393	2.05	35.0	35.0	0.11	0.09	0.638	0.514
			Re = 75,000				
107	3.65	0.0	0.0	-0.01	0.02	-0.018	0.037
110	3.65	5.0	5.0	0.11	0.02	0.190	0.038
114	3.65	10.0	10.0	0.24	0.04	0.424	0.075
118	3.65	15.0	14.9	0.36	0.10	0.636	0.172
122	3.65	20.0	19.9	0.45	0.16	0.798	0.280
387	3.67	22.0	21.9	0.47	0.20	0.814	0.347
126	3.65	25.0	24.9	0.49	0.22	0.865	0.384
130	3.65	30.0	29.9	0.43	0.25	0.758	0.432
134	3.65	35.0	34.9	0.42	0.29	0.732	0.514
			Re = 100,000				
108	4.85	0.0	0.0	-0.01	0.03	-0.008	0.032
111	4.85	5.0	5.0	0.20	0.04	0.199	0.039
115	4.85	10.0	9.9	0.41	0.07	0.405	0.072
119	4.85	15.0	14.9	0.64	0.17	0.635	0.171
123	4.85	20.0	19.9	0.78	0.28	0.776	0.276
382	4.89	20.0	19.9	0.77	0.30	0.758	0.293
388	4.89	22.0	21.9	0.81	0.34	0.791	0.337
127	4.85	25.0	24.9	0.84	0.37	0.839	0.370
384	4.90	25.0	24.9	0.73	0.38	0.713	0.370
131	4.85	30.0	29.9	0.69	0.41	0.688	0.404
135	4.85	35.0	34.9	0.68	0.49	0.677	0.486

Table 2b (Concluded)

Flat plate section, aspect ratio 1, with Hama strips.

Run no.	Speed fps	α set	α corr.	Lift lb	Drag lb	C_L	C_D	
			Re = 125,000					
109	6.07	0.0	0.0	-0.01	0.05	-0.005	0.029	
112	6.07	5.0	5.0	0.29	0.06	0.185	0.036	
116	6.08	10.0	9.9	0.62	0.11	0.396	0.071	
120	6.07	15.0	14.8	0.97	0.26	0.616	0.168	
124	6.07	20.0	19.8	1.20	0.42	0.764	0.270	
389	6.12	22.0	21.8	1.24	0.53	0.776	0.333	
128	6.07	25.0	24.8	1.25	0.56	0.795	0.359	
132	6.07	30.0	29.8	1.04	0.61	0.663	0.392	
136	6.06	35.0	34.8	1.03	0.75	0.660	0.480	
			Re = 150,000					
105	7.28	0.0	0.0	0.00	0.06	0.001	0.027	
103	7.27	0.0	0.0	-0.02	0.10	-0.007	0.044	*
104	7.26	0.0	0.0	0.01	0.10	0.004	0.043	*
101	7.27	0.0	0.0	0.02	0.12	0.010	0.053	**
102	7.28	0.0	0.0	0.02	0.12	0.011	0.053	**
106	7.27	0.0	0.0	-0.01	0.06	-0.003	0.027	
113	7.28	5.0	4.9	0.39	0.08	0.172	0.034	
117	7.28	10.0	9.9	0.85	0.15	0.377	0.066	
121	7.28	15.0	14.8	1.33	0.36	0.591	0.162	
125	7.27	20.0	19.7	1.71	0.61	0.759	0.270	
390	7.33	22.0	21.7	1.74	0.74	0.761	0.326	
129	7.28	25.0	24.7	1.73	0.79	0.767	0.352	
385	7.39	25.0	24.7	1.56	0.82	0.673	0.351	
133	7.28	30.0	29.8	1.49	0.88	0.660	0.389	
137	7.27	35.0	34.8	1.44	1.06	0.642	0.470	

* Double thickness Hama strip (0.028 in)
** Triple thickness Hama strip (0.042 in)

Table 3a

Flat plate section, aspect ratio 1.5.

Run no.	Speed fps	α set	α corr.	Lift lb	Drag lb	C_L	C_D
			Re = 42,000				
257	2.49	0.0	0.0	0.02	0.01	0.061	0.034
250	2.49	5.0	5.0	0.08	0.02	0.306	0.066
248	2.49	10.0	10.0	0.14	0.03	0.529	0.119
247	2.49	15.0	15.0	0.20	0.06	0.755	0.230
244	2.49	20.0	20.0	0.22	0.09	0.832	0.356
266	2.50	25.0	25.0	0.20	0.11	0.746	0.398
268	2.50	30.0	30.0	0.19	0.12	0.715	0.460
269	2.50	35.0	35.0	0.19	0.15	0.698	0.549
			Re = 75,000				
144	4.45	0.0	0.0	0.02	0.02	0.019	0.021
186	4.45	5.0	5.0	0.22	0.04	0.266	0.048
190	4.45	5.0	5.0	0.22	0.04	0.262	0.049
252	4.45	5.0	5.0	0.26	0.05	0.307	0.054
179	4.45	10.0	9.9	0.44	0.09	0.526	0.104
191	4.46	10.0	9.9	0.44	0.08	0.523	0.099
174	4.46	15.0	14.9	0.60	0.18	0.715	0.211
173	4.45	20.0	19.9	0.69	0.27	0.819	0.322
161	4.45	25.0	24.9	0.64	0.34	0.763	0.399
156	4.45	30.0	29.9	0.55	0.35	0.650	0.418
147	4.45	35.0	34.9	0.58	0.42	0.681	0.492
			Re = 100,000				
145	5.93	0.0	0.0	0.02	0.03	0.015	0.021
187	5.93	5.0	4.9	0.43	0.07	0.287	0.048
253	5.93	5.0	4.9	0.47	0.08	0.317	0.051
180	5.93	10.0	9.9	0.79	0.15	0.528	0.103
175	5.93	15.0	14.8	1.07	0.31	0.712	0.208
1008	6.23	18.0	17.8	1.26	0.45	0.764	0.274
172	5.93	20.0	19.8	1.21	0.47	0.808	0.316
160	5.93	25.0	24.8	1.14	0.58	0.760	0.390
155	5.93	30.0	29.8	0.94	0.60	0.629	0.402
148	5.93	35.0	34.8	0.97	0.72	0.647	0.480

Table 3a (Concluded)

Flat plate section, aspect ratio 1.5.

Run no.	Speed fps	α set	α corr.	Lift lb	Drag lb	C_L	C_D
			Re = 125,000				
146	7.42	0.0	0.0	0.03	0.05	0.014	0.020
188	7.42	5.0	4.9	0.71	0.11	0.304	0.046
254	7.41	5.0	4.9	0.77	0.12	0.330	0.050
181	7.41	10.0	9.8	1.25	0.24	0.535	0.103
177	7.42	15.0	14.7	1.69	0.50	0.723	0.215
171	7.41	20.0	19.7	1.88	0.74	0.806	0.316
159	7.42	25.0	24.7	1.78	0.90	0.759	0.385
154	7.41	30.0	29.8	1.47	0.94	0.630	0.402
149	7.42	35.0	34.8	1.46	1.11	0.623	0.475
			Re = 150,000				
143	8.91	0.0	0.0	0.01	0.07	0.002	0.020
1006	9.30	0.0	0.0	0.00	0.08	0.001	0.022
189	8.91	5.0	4.8	1.07	0.15	0.318	0.045
251	8.91	5.0	4.8	1.13	0.16	0.335	0.048
182	8.91	10.0	9.7	1.81	0.35	0.537	0.103
249	8.90	10.0	9.7	1.86	0.38	0.553	0.114
178	8.90	15.0	14.6	2.43	0.72	0.722	0.214
246	8.90	15.0	14.6	2.41	0.74	0.716	0.219
1007	9.30	18.0	17.5	2.82	1.01	0.767	0.273
162	8.90	20.0	19.6	2.70	1.06	0.801	0.313
163	8.92	20.0	19.6	2.70	1.06	0.799	0.314
164	8.90	20.0	19.6	2.66	1.05	0.789	0.313
165	8.90	20.0	19.6	2.62	1.04	0.777	0.309
166	8.90	20.0	19.6	2.65	1.05	0.786	0.311
167	8.92	20.0	19.6	2.67	1.06	0.791	0.312
168	8.91	20.0	19.6	2.67	1.05	0.791	0.311
169	8.91	20.0	19.6	2.70	1.06	0.799	0.314
170	8.88	20.0	19.6	2.66	1.05	0.794	0.314
242	8.90	20.0	19.6	2.45	1.04	0.727	0.309
243	8.90	20.0	19.6	2.43	1.04	0.720	0.307
245	8.90	20.0	19.6	2.45	1.04	0.725	0.308
265	8.90	20.0	19.6	2.56	1.08	0.758	0.319
158	8.90	25.0	24.6	2.48	1.27	0.737	0.378
152	8.90	30.0	29.7	2.06	1.33	0.610	0.393
153	8.91	30.0	29.7	2.07	1.34	0.614	0.396
151	8.90	35.0	34.7	2.02	1.54	0.599	0.455

Table 3b

Flat plate section, aspect ratio 1.5, with Hama strips.

Run no.	Speed fps	α set	α corr.	Lift lb	Drag lb	C_L	C_D
			Re = 42,000				
207	2.49	0.0	0.0	0.01	0.01	0.039	0.041
196	2.49	5.0	5.0	0.07	0.02	0.271	0.068
208	2.49	10.0	10.0	0.14	0.02	0.540	0.092
215	2.49	15.0	15.0	0.19	0.06	0.734	0.213
221	2.49	20.0	20.0	0.23	0.09	0.862	0.335
226	2.49	25.0	25.0	0.21	0.10	0.809	0.398
233	2.49	30.0	30.0	0.17	0.12	0.660	0.466
236	2.49	35.0	35.0	0.18	0.15	0.672	0.562
			Re = 75,000				
193	4.45	0.0	0.0	0.00	0.03	0.002	0.036
197	4.45	5.0	5.0	0.22	0.04	0.259	0.053
209	4.45	10.0	9.9	0.44	0.08	0.522	0.091
216	4.45	15.0	14.9	0.59	0.18	0.705	0.214
222	4.45	20.0	19.9	0.66	0.27	0.788	0.323
227	4.45	25.0	24.9	0.62	0.32	0.735	0.384
231	4.45	30.0	29.9	0.55	0.37	0.647	0.436
237	4.45	35.0	34.9	0.55	0.45	0.649	0.528
			Re = 100,000				
194	5.93	0.0	0.0	0.00	0.05	0.000	0.034
198	5.93	5.0	4.9	0.35	0.07	0.237	0.047
210	5.93	10.0	9.9	0.75	0.13	0.504	0.090
217	5.93	15.0	14.8	1.07	0.32	0.711	0.216
223	5.92	20.0	19.8	1.14	0.48	0.765	0.321
228	5.93	25.0	24.8	1.08	0.57	0.719	0.378
232	5.93	30.0	29.9	0.93	0.63	0.623	0.423
238	5.93	35.0	34.9	0.93	0.76	0.620	0.508
			Re = 125,000				
195	7.42	0.0	0.0	-0.01	0.08	-0.002	0.034
199	7.41	5.0	4.9	0.55	0.10	0.235	0.044
212	7.41	10.0	9.8	1.13	0.21	0.485	0.091
218	7.41	15.0	14.7	1.59	0.49	0.681	0.211
224	7.41	20.0	19.7	1.71	0.73	0.734	0.311
229	7.41	25.0	24.7	1.64	0.87	0.701	0.374
234	7.41	30.0	29.8	1.43	0.98	0.612	0.420
239	7.41	35.0	34.8	1.42	1.18	0.611	0.506

Table 3b (Concluded)

Flat plate section, aspect ratio 1.5, with Hama strips.

Run no.	Speed fps	α set	α corr.	Lift lb	Drag lb	C_L	C_D
			Re = 150,000				
192	8.90	0.0	0.0	-0.01	0.11	-0.002	0.032
202	8.92	5.0	4.9	0.75	0.14	0.223	0.041
213	8.90	10.0	9.8	1.49	0.28	0.442	0.084
214	8.92	10.0	9.8	1.49	0.28	0.441	0.082
219	8.91	15.0	14.7	2.11	0.67	0.624	0.200
220	8.88	15.0	14.7	2.11	0.67	0.627	0.199
1009	9.31	18.0	17.6	2.50	0.94	0.677	0.256
225	8.92	20.0	19.6	2.25	0.99	0.666	0.292
241	8.90	20.0	19.6	2.24	0.98	0.667	0.292
1010	9.30	22.0	21.6	2.57	1.19	0.697	0.322
230	8.91	25.0	24.7	2.10	1.18	0.622	0.350
235	8.89	30.0	29.7	1.96	1.37	0.584	0.407
240	8.89	35.0	34.7	2.01	1.68	0.597	0.501

Table 3c

Flat plate section, aspect ratio 1.5, with trip wire.

Run no.	Speed fps	Re x10	α set	α corr.	Lift lb	Drag lb	C_L	C_D
400	2.52	42	5.0	5.0	0.08	0.02	0.284	0.081
395	2.49	42	10.0	10.0	0.14	0.03	0.511	0.124
404	4.48	75	5.0	5.0	0.22	0.06	0.256	0.073
396	4.45	75	10.0	9.9	0.42	0.10	0.499	0.123
403	5.96	100	5.0	4.9	0.33	0.10	0.221	0.069
397	5.92	100	10.0	9.9	0.70	0.18	0.468	0.119
402	7.45	125	5.0	4.9	0.44	0.16	0.186	0.066
398	7.44	125	10.0	9.8	1.01	0.27	0.429	0.114
394	8.90	150	0.0	0.0	0.00	0.18	0.001	0.054
401	8.95	150	5.0	4.9	0.55	0.22	0.162	0.064
399	8.95	150	10.0	9.8	1.39	0.38	0.406	0.110

0.03 in diameter, 5% local chord aft of leading edge.

Table 4a

Flat plate section, aspect ratio 2.

Run no.	Speed fps	α set	α corr.	Lift lb	Drag lb	C_L	C_D
			Re = 42,000				
275	2.89	0.0	0.0	0.01	0.01	0.022	0.038
283	2.89	5.0	5.0	0.12	0.02	0.336	0.050
288	2.89	10.0	10.0	0.21	0.04	0.595	0.106
1019	3.03	15.0	15.0	0.30	0.09	0.769	0.223
300	2.89	20.0	20.0	0.27	0.12	0.764	0.328
314	2.89	22.0	22.0	0.27	0.12	0.748	0.331
309	2.89	25.0	25.0	0.26	0.13	0.718	0.375
315	2.89	30.0	30.0	0.25	0.17	0.689	0.471
322	2.89	35.0	35.0	0.25	0.19	0.707	0.528
			Re = 75,000				
276	5.15	0.0	0.0	0.01	0.03	0.008	0.026
284	5.18	5.0	4.9	0.38	0.05	0.336	0.048
289	5.18	10.0	9.9	0.66	0.11	0.579	0.098
1018	5.40	15.0	14.9	0.91	0.28	0.734	0.225
301	5.18	20.0	19.9	0.82	0.35	0.720	0.307
328	5.18	22.0	21.9	0.80	0.38	0.702	0.334
310	5.17	25.0	24.9	0.72	0.39	0.630	0.347
316	5.18	30.0	29.9	0.70	0.49	0.617	0.428
323	5.18	35.0	34.9	0.72	0.57	0.632	0.498
			Re = 100,000				
277	6.88	0.0	0.0	0.03	0.05	0.014	0.026
285	6.91	5.0	4.9	0.71	0.10	0.352	0.049
290	6.90	10.0	9.8	1.21	0.20	0.597	0.100
1017	7.18	15.0	14.7	1.67	0.50	0.760	0.277
308	6.90	18.0	17.7	1.56	0.56	0.769	0.276
302	6.90	20.0	19.8	1.44	0.61	0.711	0.301
329	6.90	22.0	21.8	1.38	0.66	0.682	0.325
311	6.90	25.0	24.8	1.23	0.69	0.608	0.339
317	6.90	30.0	29.8	1.22	0.84	0.602	0.414
324	6.91	35.0	34.8	1.25	1.00	0.615	0.492

Table 4a (Concluded)

Flat plate section, aspect ratio 2.

Run no.	Speed fps	α set	α corr.	Lift lb	Drag lb	C_L	C_D
			Re = 125,000				
282	8.62	0.0	0.0	0.02	0.07	0.006	0.023
286	8.63	5.0	4.8	1.17	0.15	0.370	0.046
291	8.62	10.0	9.7	1.92	0.31	0.607	0.099
1016	8.97	15.0	14.6	2.55	0.76	0.743	0.221
303	8.63	20.0	19.6	2.26	0.94	0.713	0.298
330	8.62	22.0	21.7	2.12	1.01	0.671	0.320
312	8.62	25.0	24.7	1.89	1.06	0.598	0.334
318	8.63	30.0	29.7	1.89	1.30	0.598	0.409
325	8.60	35.0	34.7	1.90	1.53	0.603	0.485
			Re = 150,000				
274	10.31	0.0	0.0	0.02	0.11	0.005	0.023
1011	10.76	0.0	0.0	0.02	0.09	0.005	0.018
287	10.32	5.0	4.7	1.68	0.21	0.371	0.046
292	10.35	10.0	9.5	2.80	0.46	0.614	0.101
1012	10.77	12.0	11.5	3.29	0.72	0.667	0.146
1013	10.77	14.0	13.4	3.58	0.88	0.725	0.179
1015	10.76	15.0	14.4	3.65	1.06	0.742	0.216
1014	10.78	16.0	15.4	3.68	1.17	0.745	0.236
307	10.35	18.0	17.5	3.39	1.23	0.745	0.269
304	10.35	20.0	19.5	2.89	1.25	0.634	0.275
305	10.34	20.0	19.5	2.96	1.28	0.650	0.282
306	10.36	20.0	19.5	2.95	1.29	0.647	0.282
313	10.34	25.0	24.6	2.67	1.48	0.588	0.326
321	10.34	30.0	29.6	2.72	1.84	0.599	0.405
327	10.36	35.0	34.6	2.74	2.25	0.601	0.492

Table 4b

Flat plate section, aspect ratio 2, with Hama strips.

Run no.	Speed fps	α set	α corr.	Lift lb	Drag lb	C_L	C_D
			Re = 42,000				
416	2.92	0.0	0.0	0.01	0.02	0.016	0.046
417	2.92	5.0	5.0	0.12	0.02	0.338	0.064
422	2.92	10.0	10.0	0.23	0.04	0.621	0.106
427	2.92	15.0	15.0	0.29	0.08	0.789	0.212
455	2.92	18.0	18.0	0.30	0.10	0.835	0.283
432	2.92	20.0	20.0	0.30	0.12	0.837	0.325
445	2.92	30.0	30.0	0.26	0.17	0.731	0.471
450	2.92	35.0	35.0	0.27	0.21	0.744	0.566
			Re = 75,000				
415	5.24	0.0	0.0	0.01	0.04	0.008	0.037
418	5.24	5.0	4.9	0.36	0.07	0.310	0.056
423	5.23	10.0	9.9	0.69	0.12	0.589	0.099
428	5.23	15.0	14.9	0.86	0.25	0.737	0.213
433	5.23	20.0	19.9	0.88	0.36	0.758	0.313
440	5.23	25.0	24.9	0.78	0.42	0.669	0.365
446	5.23	30.0	29.9	0.75	0.51	0.645	0.436
451	5.23	35.0	34.9	0.76	0.61	0.649	0.524
			Re = 100,000				
414	6.95	0.0	0.0	0.00	0.07	0.001	0.035
419	6.96	5.0	4.9	0.57	0.10	0.275	0.051
424	6.95	10.0	9.8	1.12	0.19	0.543	0.090
429	6.96	15.0	14.8	1.48	0.43	0.719	0.210
434	6.96	20.0	19.8	1.49	0.63	0.725	0.306
441	6.95	25.0	24.8	1.32	0.74	0.640	0.358
447	6.95	30.0	29.8	1.26	0.87	0.615	0.423
452	6.95	35.0	34.8	1.26	1.04	0.611	0.505
			Re = 125,000				
413	8.66	0.0	0.0	0.00	0.11	0.000	0.034
420	8.66	5.0	4.9	0.73	0.15	0.229	0.046
425	8.67	10.0	9.8	1.54	0.26	0.482	0.081
430	8.68	15.0	14.7	2.08	0.63	0.648	0.195
435	8.66	20.0	19.7	2.06	0.90	0.646	0.282
442	8.66	25.0	24.7	1.86	1.08	0.583	0.339
448	8.66	30.0	29.7	1.85	1.30	0.579	0.408
453	8.66	35.0	34.7	1.86	1.57	0.581	0.493

Table 4b (Concluded)

Flat plate section, aspect ratio 2, with Hama strips.

Run no.	Speed fps	α set	α corr.	Lift lb	Drag lb	C_L	C_D
			Re = 150,000				
412	10.37	0.0	0.0	0.03	0.15	0.007	0.032
421	10.40	5.0	4.8	1.00	0.20	0.218	0.044
426	10.40	10.0	9.7	2.12	0.35	0.461	0.076
431	10.36	15.0	14.5	2.88	0.87	0.630	0.190
456	10.40	18.0	17.5	2.92	1.12	0.635	0.244
438	10.42	20.0	19.6	2.78	1.26	0.602	0.273
444	10.40	25.0	24.6	2.46	1.48	0.534	0.322
449	10.42	30.0	29.6	2.54	1.84	0.549	0.398
454	10.41	35.0	34.6	2.56	2.22	0.556	0.482

Table 5a

NACA 0015 section, aspect ratio 1.

Run no.	Speed fps	α set	α corr.	Lift lb	Drag lb	C_L	C_D
			Re = 42,000				
594	2.07	0.0	0.0	0.00	0.01	0.000	0.028
590	2.07	5.0	5.0	0.04	0.01	0.234	0.042
585	2.07	10.0	10.0	0.07	0.01	0.410	0.076
599	2.07	15.0	15.0	0.10	0.02	0.556	0.133
605	2.07	20.0	20.0	0.13	0.04	0.717	0.241
611	2.07	25.0	25.0	0.15	0.07	0.821	0.366
631	2.07	27.0	27.0	0.12	0.07	0.675	0.373
618	2.07	30.0	30.0	0.11	0.08	0.623	0.427
624	2.07	35.0	35.0	0.11	0.09	0.607	0.495
			Re = 75,000				
595	3.68	0.0	0.0	0.00	0.01	0.003	0.022
591	3.68	5.0	5.0	0.13	0.02	0.230	0.038
586	3.68	10.0	10.0	0.23	0.04	0.399	0.074
601	3.68	15.0	14.9	0.34	0.07	0.583	0.129
606	3.68	20.0	19.9	0.41	0.15	0.714	0.252
612	3.68	25.0	24.9	0.46	0.22	0.795	0.374
632	3.68	27.0	26.9	0.34	0.21	0.594	0.372
633	3.68	27.0	26.9	0.35	0.21	0.614	0.371
634	3.68	27.0	26.9	0.34	0.21	0.586	0.367
619	3.68	30.0	29.9	0.35	0.24	0.610	0.424
625	3.68	35.0	34.9	0.37	0.30	0.639	0.517
			Re = 100,000				
596	4.90	0.0	0.0	0.00	0.02	0.001	0.017
592	4.90	5.0	5.0	0.22	0.03	0.215	0.034
587	4.90	10.0	9.9	0.40	0.07	0.392	0.067
602	4.90	15.0	14.9	0.58	0.12	0.571	0.121
607	4.90	20.0	19.9	0.72	0.25	0.707	0.243
613	4.91	25.0	24.9	0.78	0.37	0.764	0.365
637	4.91	27.0	26.9	0.58	0.36	0.565	0.351
620	4.90	30.0	29.9	0.57	0.41	0.562	0.400
626	4.91	35.0	34.9	0.60	0.50	0.586	0.486
636	4.90	35.0	34.9	0.61	0.49	0.592	0.482

Table 5a (Concluded)

NACA 0015 section, aspect ratio 1.

Run no.	Speed fps	α set	α corr.	Lift lb	Drag lb	C_L	C_D
			Re = 125,000				
597	6.15	0.0	0.0	-0.01	0.03	-0.005	0.017
593	6.14	5.0	4.9	0.32	0.05	0.200	0.030
588	6.14	10.0	9.9	0.65	0.10	0.406	0.064
603	6.15	15.0	14.9	0.93	0.18	0.577	0.114
608	6.14	20.0	19.8	1.09	0.41	0.682	0.255
614	6.14	25.0	24.8	1.10	0.56	0.687	0.347
638	6.14	27.0	26.9	0.87	0.56	0.544	0.351
621	6.14	30.0	29.9	0.88	0.62	0.547	0.387
627	6.15	35.0	34.9	0.92	0.77	0.571	0.480
			Re = 150,000				
582	7.35	0.0	0.0	-0.02	0.05	-0.007	0.020
583	7.35	0.0	0.0	0.01	0.05	0.005	0.021
589	7.35	5.0	4.9	0.45	0.07	0.194	0.029
584	7.36	10.0	9.8	0.94	0.14	0.407	0.063
598	7.36	10.0	9.9	0.90	0.14	0.392	0.061
604	7.36	10.0	9.8	0.94	0.14	0.410	0.060
610	7.35	10.0	9.9	0.93	0.14	0.403	0.060
617	7.36	10.0	9.9	0.93	0.14	0.404	0.060
623	7.35	10.0	9.9	0.92	0.14	0.399	0.060
629	7.35	10.0	9.9	0.93	0.14	0.404	0.062
635	7.36	10.0	9.8	0.94	0.14	0.406	0.063
639	7.36	10.0	9.9	0.91	0.14	0.395	0.062
600	7.35	15.0	14.8	1.32	0.27	0.573	0.119
609	7.36	20.0	19.7	1.56	0.56	0.678	0.245
615	7.34	25.0	24.7	1.65	0.79	0.721	0.345
616	7.35	25.0	24.7	1.60	0.79	0.697	0.344
630	7.35	27.0	26.8	1.21	0.79	0.525	0.345
622	7.35	30.0	29.8	1.19	0.87	0.518	0.379
628	7.35	35.0	34.8	1.30	1.08	0.567	0.471

Table 5b

NACA 0015 section, aspect ratio 1, with Hama strips.

Run no.	Speed fps	α set	α corr.	Lift lb	Drag lb	C_L	C_D
			Re = 42,000				
641	2.07	0.0	0.0	0.00	0.01	0.019	0.036
645	2.07	5.0	5.0	0.03	0.01	0.182	0.043
650	2.07	10.0	10.0	0.07	0.01	0.389	0.078
655	2.07	15.0	15.0	0.09	0.03	0.511	0.139
660	2.07	20.0	20.0	0.12	0.04	0.683	0.227
666	2.07	25.0	25.0	0.15	0.06	0.803	0.354
685	2.07	27.0	27.0	0.12	0.07	0.640	0.387
675	2.07	30.0	30.0	0.11	0.08	0.613	0.425
680	2.07	35.0	35.0	0.11	0.09	0.615	0.509
			Re = 75,000				
642	3.68	0.0	0.0	-0.01	0.02	-0.012	0.034
646	3.68	5.0	5.0	0.10	0.03	0.176	0.045
651	3.68	10.0	10.0	0.22	0.04	0.376	0.075
656	3.68	15.0	15.0	0.31	0.08	0.539	0.139
661	3.68	20.0	19.9	0.41	0.13	0.704	0.218
662	3.68	20.0	19.9	0.41	0.13	0.715	0.220
667	3.68	25.0	24.9	0.47	0.22	0.810	0.374
671	3.68	25.0	24.9	0.47	0.22	0.821	0.379
686	3.68	27.0	26.9	0.36	0.22	0.628	0.387
676	3.68	30.0	29.9	0.35	0.25	0.608	0.427
681	3.68	35.0	34.9	0.36	0.30	0.631	0.515
			Re = 100,000				
643	4.90	0.0	0.0	-0.01	0.03	-0.011	0.032
647	4.90	5.0	5.0	0.18	0.04	0.171	0.040
652	4.90	10.0	9.9	0.38	0.07	0.368	0.072
657	4.90	15.0	14.9	0.56	0.13	0.550	0.126
663	4.90	20.0	19.9	0.73	0.21	0.714	0.204
672	4.90	25.0	24.9	0.80	0.37	0.780	0.364
687	4.90	27.0	26.9	0.58	0.36	0.563	0.357
677	4.90	30.0	29.9	0.58	0.41	0.568	0.401
682	4.90	35.0	34.9	0.59	0.49	0.580	0.477

Table 5b (Concluded)

NACA 0015 section, aspect ratio 1, with Hama strips.

Run no.	Speed fps	α set	α corr.	Lift lb	Drag lb	C_L	C_D	
			Re = 125,000					
644	6.15	0.0	0.0	-0.01	0.05	-0.005	0.028	
648	6.14	5.0	5.0	0.27	0.06	0.168	0.040	
653	6.14	10.0	9.9	0.59	0.11	0.366	0.069	
658	6.14	15.0	14.9	0.90	0.19	0.563	0.120	
664	6.14	20.0	19.8	1.16	0.31	0.723	0.193	
673	6.14	25.0	24.8	1.22	0.59	0.762	0.369	
688	6.15	27.0	26.9	0.87	0.56	0.540	0.347	
678	6.13	30.0	29.9	0.88	0.63	0.547	0.395	
683	6.14	35.0	34.9	0.91	0.76	0.568	0.476	
			Re = 150,000					
640	7.36	0.0	0.0	0.01	0.06	0.003	0.028	
690	7.36	0.0	0.0	-0.01	0.10	-0.003	0.042	*
691	7.35	0.0	0.0	0.01	0.13	0.004	0.058	**
649	7.35	5.0	4.9	0.44	0.09	0.191	0.039	
654	7.35	10.0	9.9	0.87	0.15	0.377	0.067	
659	7.36	15.0	14.8	1.28	0.28	0.558	0.122	
665	7.36	20.0	19.7	1.60	0.41	0.695	0.179	
674	7.37	25.0	24.7	1.71	0.88	0.740	0.380	
689	7.35	27.0	26.8	1.22	0.81	0.531	0.351	
679	7.35	30.0	29.8	1.22	0.90	0.531	0.392	
684	7.36	35.0	34.8	1.29	1.08	0.558	0.471	

* Double thickness Hama strip (0.028 in)
** Triple thickness Hama strip (0.042 in)

Table 6a

NACA 0015 section, aspect ratio 1.5.

Run no.	Speed fps	α set	α corr.	Lift lb	Drag lb	C_L	C_D
			Re = 42,000				
762	2.58	0.0	0.0	0.00	0.01	0.006	0.041
766	2.58	5.0	5.0	0.07	0.02	0.257	0.057
771	2.58	10.0	10.0	0.14	0.03	0.490	0.089
776	2.58	15.0	15.0	0.19	0.04	0.680	0.156
865	2.60	17.0	17.0	0.19	0.07	0.648	0.240
781	2.58	20.0	20.0	0.21	0.08	0.736	0.295
786	2.58	25.0	25.0	0.22	0.11	0.786	0.397
791	2.58	30.0	30.0	0.22	0.13	0.780	0.474
796	2.58	35.0	35.0	0.20	0.15	0.705	0.536
			Re = 75,000				
763	4.66	0.0	0.0	0.00	0.02	0.000	0.027
767	4.63	5.0	5.0	0.25	0.04	0.269	0.043
772	4.63	10.0	9.9	0.43	0.07	0.474	0.076
777	4.63	15.0	14.9	0.58	0.14	0.635	0.150
861	4.65	15.0	14.9	0.58	0.14	0.631	0.154
864	4.65	17.0	16.9	0.57	0.21	0.615	0.228
782	4.63	20.0	19.9	0.62	0.25	0.678	0.278
787	4.63	25.0	24.9	0.65	0.33	0.708	0.363
792	4.63	30.0	29.9	0.58	0.39	0.633	0.430
797	4.63	35.0	34.9	0.57	0.45	0.624	0.490
			Re = 100,000				
764	6.18	0.0	0.0	0.00	0.04	0.002	0.023
768	6.18	5.0	4.9	0.40	0.06	0.248	0.036
773	6.17	10.0	9.9	0.75	0.12	0.462	0.072
778	6.18	15.0	14.8	1.03	0.23	0.633	0.142
863	6.21	17.0	16.8	1.01	0.36	0.614	0.221
783	6.17	20.0	19.8	1.10	0.45	0.677	0.276
788	6.18	25.0	24.8	1.09	0.57	0.674	0.349
793	6.17	30.0	29.8	0.98	0.67	0.604	0.410
798	6.17	35.0	34.8	0.95	0.76	0.584	0.470

Table 6a (Concluded)

NACA 0015 section, aspect ratio 1.5.

Run no.	Speed fps	α set	α corr.	Lift lb	Drag lb	C_L	C_D
			Re = 125,000				
765	7.67	0.0	0.0	0.00	0.05	0.000	0.021
769	7.69	5.0	4.9	0.60	0.09	0.237	0.035
774	7.67	10.0	9.8	1.16	0.17	0.461	0.070
779	7.68	15.0	14.7	1.58	0.33	0.631	0.130
862	7.72	17.0	16.8	1.52	0.55	0.600	0.218
784	7.69	20.0	19.7	1.66	0.68	0.658	0.269
789	7.68	25.0	24.7	1.64	0.86	0.654	0.342
794	7.68	30.0	29.8	1.51	1.02	0.600	0.404
799	7.68	35.0	34.8	1.42	1.17	0.568	0.465
			Re = 150,000				
761	9.20	0.0	0.0	0.00	0.07	0.000	0.019
770	9.21	5.0	4.9	0.86	0.12	0.239	0.033
775	9.18	10.0	9.7	1.64	0.24	0.457	0.067
780	9.20	15.0	14.6	2.37	0.44	0.656	0.122
860	9.29	15.0	14.6	2.38	0.45	0.649	0.123
859	9.27	16.0	15.6	2.26	0.69	0.619	0.188
858	9.25	18.0	17.6	2.31	0.86	0.634	0.237
785	9.20	20.0	19.6	2.34	0.96	0.649	0.266
790	9.19	25.0	24.6	2.29	1.21	0.637	0.337
795	9.18	30.0	29.7	2.00	1.38	0.557	0.386
801	9.19	35.0	34.7	1.99	1.66	0.553	0.461

Table 6b

NACA 0015 section, aspect ratio 1.5, with Hama strips.

Run no.	Speed fps	α set	α corr.	Lift lb	Drag lb	C_L	C_D
			Re = 42,000				
802	2.58	0.0	0.0	0.00	0.01	0.016	0.052
807	2.58	5.0	5.0	0.07	0.02	0.251	0.067
812	2.58	10.0	10.0	0.13	0.03	0.463	0.113
817	2.58	15.0	15.0	0.18	0.04	0.652	0.157
839	2.58	18.0	18.0	0.20	0.07	0.707	0.250
822	2.58	20.0	20.0	0.21	0.09	0.736	0.304
827	2.58	25.0	25.0	0.23	0.11	0.796	0.390
832	2.58	30.0	30.0	0.22	0.14	0.774	0.478
843	2.58	35.0	35.0	0.20	0.15	0.701	0.544
			Re = 75,000				
803	4.63	0.0	0.0	0.01	0.03	0.011	0.036
808	4.63	5.0	5.0	0.21	0.05	0.231	0.051
813	4.63	10.0	9.9	0.41	0.08	0.447	0.087
818	4.63	15.0	14.9	0.60	0.12	0.656	0.137
840	4.63	18.0	17.9	0.61	0.22	0.663	0.239
823	4.63	20.0	19.9	0.61	0.25	0.675	0.278
828	4.63	25.0	24.9	0.63	0.32	0.695	0.356
833	4.63	30.0	29.9	0.61	0.39	0.665	0.423
844	4.63	35.0	34.9	0.57	0.45	0.623	0.495
			Re = 100,000				
804	6.17	0.0	0.0	0.02	0.05	0.014	0.034
809	6.17	5.0	4.9	0.38	0.08	0.233	0.048
814	6.17	10.0	9.9	0.70	0.13	0.430	0.081
819	6.17	15.0	14.8	1.04	0.21	0.644	0.130
841	6.18	18.0	17.8	1.19	0.32	0.733	0.198
824	6.18	20.0	19.8	1.09	0.44	0.672	0.270
829	6.17	25.0	24.8	1.09	0.56	0.673	0.345
834	6.17	30.0	29.8	1.00	0.66	0.618	0.408
845	6.17	35.0	34.8	0.97	0.78	0.598	0.478

Table 6b (Concluded)

NACA 0015 section, aspect ratio 1.5, with Hama strips.

Run no.	Speed fps	α set	α corr.	Lift lb	Drag lb	C_L	C_D
			Re = 125,000				
805	7.68	0.0	0.0	0.03	0.08	0.012	0.033
810	7.66	5.0	4.9	0.58	0.11	0.231	0.045
815	7.69	10.0	9.8	1.07	0.20	0.427	0.079
820	7.68	15.0	14.7	1.59	0.32	0.634	0.127
842	7.69	18.0	17.7	1.93	0.41	0.766	0.162
825	7.68	20.0	19.7	1.68	0.67	0.670	0.267
830	7.68	25.0	24.7	1.64	0.86	0.652	0.342
835	7.68	30.0	29.8	1.44	0.98	0.573	0.392
846	7.69	35.0	34.8	1.46	1.18	0.580	0.470
			Re = 150,000				
806	9.23	0.0	0.0	0.05	0.11	0.013	0.031
811	9.22	5.0	4.9	0.83	0.16	0.230	0.043
816	9.19	10.0	9.8	1.55	0.27	0.430	0.076
821	9.22	15.0	14.6	2.36	0.44	0.651	0.123
838	9.23	18.0	17.5	2.82	0.57	0.778	0.157
826	9.23	20.0	19.6	2.32	0.95	0.641	0.263
837	9.23	20.0	19.6	2.38	0.95	0.658	0.261
831	9.22	25.0	24.6	2.33	1.24	0.644	0.342
836	9.23	30.0	29.7	2.06	1.42	0.569	0.392
847	9.23	35.0	34.7	2.07	1.70	0.572	0.468

Table 7a

NACA 0015 section, aspect ratio 2.

Run no.	Speed fps	α set	α corr.	Lift lb	Drag lb	C_L	C_D
			Re = 42,000				
877	3.00	0.0	0.0	0.02	0.02	0.056	0.042
878	3.00	5.0	5.0	0.12	0.02	0.321	0.055
883	3.00	10.0	10.0	0.20	0.04	0.533	0.098
888	3.00	15.0	15.0	0.26	0.07	0.688	0.187
897	3.00	20.0	20.0	0.28	0.12	0.721	0.302
901	3.00	25.0	25.0	0.30	0.15	0.781	0.395
910	3.00	30.0	30.0	0.30	0.18	0.784	0.473
917	3.00	35.0	35.0	0.28	0.21	0.722	0.556
			Re = 75,000				
875	5.36	0.0	0.0	0.01	0.03	0.008	0.026
879	5.36	5.0	4.9	0.38	0.05	0.312	0.042
884	5.36	10.0	9.9	0.62	0.10	0.505	0.078
889	5.36	15.0	14.9	0.77	0.22	0.633	0.177
898	5.36	20.0	19.9	0.80	0.35	0.658	0.283
902	5.36	25.0	24.9	0.83	0.43	0.676	0.355
911	5.36	30.0	29.9	0.77	0.51	0.629	0.416
918	5.36	35.0	34.9	0.78	0.61	0.636	0.500
			Re = 100,000				
873	7.14	0.0	0.0	0.01	0.05	0.006	0.022
880	7.14	5.0	4.9	0.65	0.08	0.299	0.039
885	7.13	10.0	9.8	1.12	0.16	0.518	0.075
923	7.14	12.0	11.8	1.33	0.20	0.611	0.093
925	7.14	13.0	12.8	1.41	0.22	0.651	0.103
926	7.14	14.0	13.8	1.45	0.28	0.668	0.128
890	7.14	15.0	14.8	1.33	0.38	0.613	0.177
899	7.15	20.0	19.8	1.38	0.59	0.637	0.273
903	7.14	25.0	24.8	1.40	0.75	0.645	0.344
912	7.14	30.0	29.8	1.30	0.87	0.600	0.400
919	7.14	35.0	34.8	1.31	1.04	0.602	0.478

Table 7a (Concluded)

NACA 0015 section, aspect ratio 2.

Run no.	Speed fps	α set	α corr.	Lift lb	Drag lb	C_L	C_D
			Re = 125,000				
872	8.92	0.0	0.0	0.01	0.06	0.003	0.019
881	8.93	5.0	4.8	0.99	0.12	0.290	0.036
886	8.90	10.0	9.7	1.76	0.24	0.522	0.072
891	8.93	15.0	14.7	2.11	0.59	0.622	0.175
900	8.93	20.0	19.7	2.15	0.93	0.633	0.274
904	8.93	25.0	24.7	2.09	1.14	0.615	0.336
913	8.93	30.0	29.7	1.89	1.31	0.557	0.387
920	8.94	35.0	34.7	1.97	1.61	0.579	0.474
			Re = 150,000				
869	10.71	0.0	0.0	0.00	0.08	0.001	0.017
876	10.70	0.0	0.0	0.00	0.08	0.000	0.017
882	10.71	5.0	4.8	1.39	0.16	0.284	0.032
887	10.70	10.0	9.6	2.49	0.32	0.510	0.066
922	10.71	12.0	11.5	2.94	0.39	0.603	0.079
924	10.71	13.0	12.5	3.13	0.45	0.641	0.092
927	10.71	14.0	13.5	3.23	0.52	0.661	0.107
892	10.51	15.0	14.5	2.84	0.80	0.604	0.169
894	10.71	15.0	14.5	2.99	0.79	0.612	0.162
928	10.70	17.0	16.5	2.88	1.02	0.592	0.210
896	10.71	20.0	19.5	3.01	1.29	0.616	0.264
909	10.70	25.0	24.6	2.70	1.52	0.555	0.313
915	10.71	30.0	29.6	2.65	1.88	0.543	0.384
916	10.71	35.0	34.6	2.78	2.31	0.570	0.473
			Re = 182,000				
907	13.01	25.0	24.4	3.81	2.23	0.529	0.310

Table 7b

NACA 0015 section, aspect ratio 2, with Hama strips.

Run no.	Speed fps	α set	α corr.	Lift lb	Drag lb	C_L	C_D
			Re = 42,000				
930	3.00	0.0	0.0	0.01	0.01	0.037	0.038
934	3.00	5.0	5.0	0.10	0.02	0.258	0.062
939	3.00	10.0	10.0	0.19	0.04	0.504	0.095
944	3.00	15.0	15.0	0.27	0.06	0.693	0.164
951	3.00	20.0	20.0	0.28	0.11	0.726	0.279
957	3.00	25.0	25.0	0.29	0.15	0.768	0.383
981	3.03	30.0	30.0	0.28	0.18	0.708	0.472
987	3.03	35.0	35.0	0.29	0.21	0.735	0.549
			Re = 75,000				
931	5.36	0.0	0.0	0.02	0.04	0.012	0.036
935	5.36	5.0	5.0	0.31	0.06	0.250	0.049
940	5.36	10.0	9.9	0.60	0.11	0.489	0.087
945	5.36	15.0	14.9	0.86	0.16	0.703	0.133
952	5.35	20.0	19.9	0.87	0.31	0.714	0.254
958	5.36	25.0	24.9	0.84	0.43	0.690	0.355
982	5.40	30.0	29.9	0.79	0.53	0.632	0.428
988	5.40	35.0	34.9	0.79	0.62	0.639	0.499
			Re = 100,000				
932	7.14	0.0	0.0	0.02	0.07	0.009	0.034
936	7.14	5.0	4.9	0.53	0.10	0.245	0.047
941	7.14	10.0	9.8	1.05	0.18	0.486	0.083
946	7.15	15.0	14.8	1.50	0.28	0.688	0.128
996	7.18	17.0	16.7	1.73	0.37	0.787	0.167
998	7.19	18.0	17.7	1.79	0.41	0.814	0.188
953	7.14	20.0	19.7	1.57	0.54	0.723	0.248
959	7.13	25.0	24.8	1.39	0.74	0.642	0.342
983	7.18	30.0	29.8	1.32	0.91	0.601	0.414
989	7.18	35.0	34.8	1.34	1.07	0.609	0.486

Table 7b (Concluded)

NACA 0015 section, aspect ratio 2, with Hama strips.

Run no.	Speed fps	α set	α corr.	Lift lb	Drag lb	C_L	C_D
			Re = 125,000				
933	8.94	0.0	0.0	0.01	0.11	0.002	0.032
937	8.92	5.0	4.9	0.82	0.15	0.243	0.045
942	8.93	10.0	9.7	1.62	0.27	0.476	0.079
947	8.92	15.0	14.6	2.33	0.43	0.688	0.128
954	8.92	20.0	19.6	2.44	0.82	0.721	0.243
960	8.92	25.0	24.7	2.04	1.12	0.603	0.331
984	8.92	30.0	29.7	1.97	1.38	0.582	0.408
991	8.97	35.0	34.7	2.00	1.63	0.584	0.477
			Re = 150,000				
929	10.71	0.0	0.0	0.01	0.13	0.002	0.027
938	10.70	5.0	4.8	1.17	0.20	0.240	0.040
943	10.68	10.0	9.6	2.33	0.37	0.481	0.077
948	10.70	15.0	14.5	3.19	0.57	0.655	0.117
950	10.70	15.0	14.5	3.09	0.57	0.634	0.118
978	10.77	15.0	14.5	3.40	0.61	0.689	0.124
964	10.69	16.0	15.5	3.41	0.69	0.700	0.141
967	10.71	16.0	15.4	3.52	0.69	0.722	0.142
968	10.67	16.0	15.5	3.23	0.64	0.667	0.131
995	10.77	17.0	16.4	3.70	0.77	0.750	0.156
997	10.77	18.0	17.4	3.84	0.86	0.777	0.173
999	10.77	19.0	18.4	3.79	1.05	0.769	0.213
955	10.71	20.0	19.5	3.40	1.14	0.696	0.233
979	10.75	20.0	19.5	3.40	1.25	0.691	0.254
963	10.71	25.0	24.6	2.68	1.52	0.549	0.312
980	10.76	25.0	24.6	2.72	1.60	0.553	0.325
986	10.78	30.0	29.5	2.81	1.95	0.568	0.394
993	10.77	35.0	34.5	2.84	2.35	0.576	0.476
			Re = 175,000				
965	12.49	16.0	15.3	4.30	1.08	0.648	0.163
956	12.50	20.0	19.3	4.47	1.64	0.672	0.247
			Re = 196,000				
966	14.00	16.0	15.2	4.88	1.43	0.585	0.171

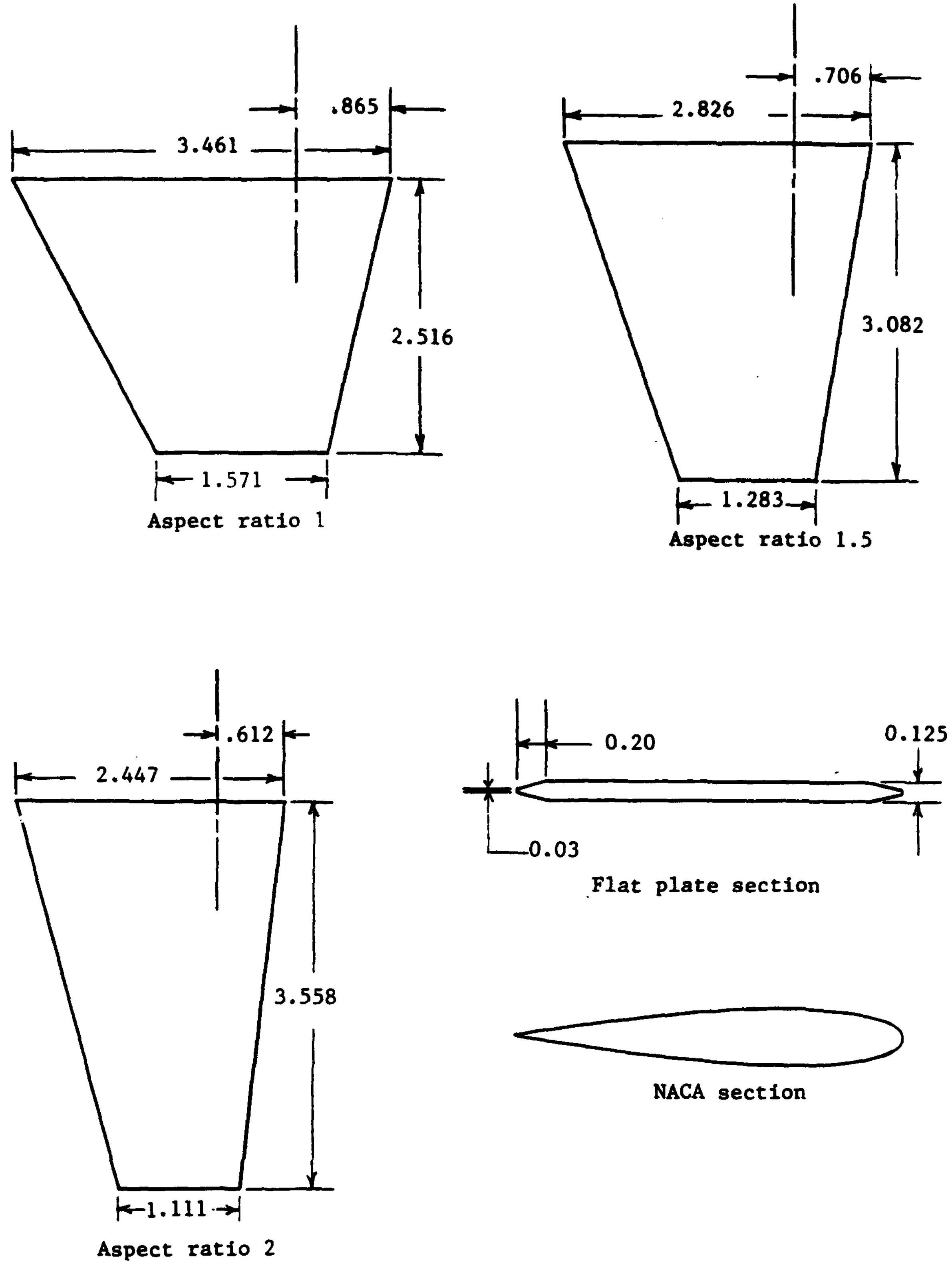

FIGURE 1 PLAN AND SECTION VIEWS OF FINS. ALL DIMENSIONS IN INCHES.

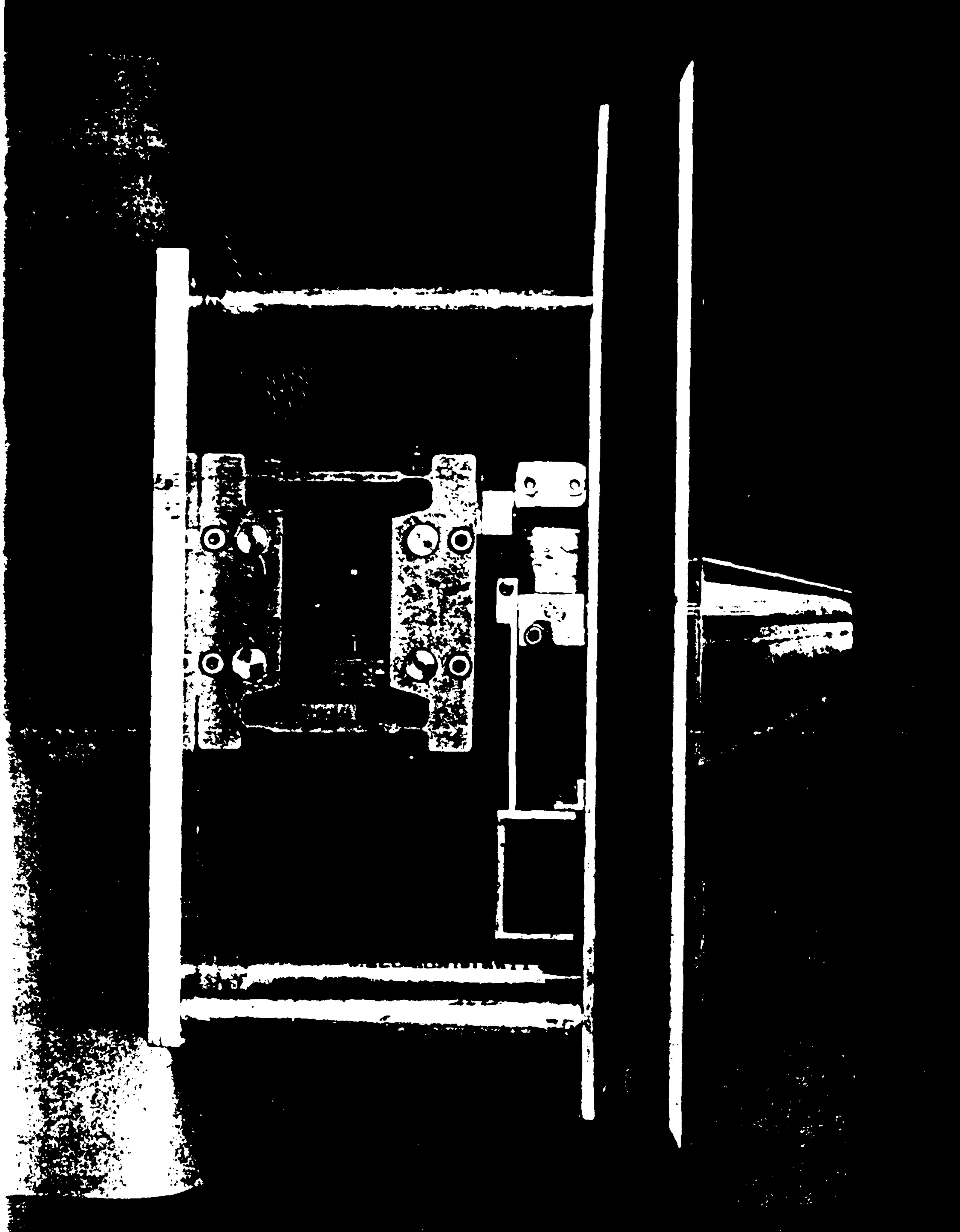

FIGURE 2 APPARATUS WITH ASPECT RATIO 1 NACA 0015 FIN

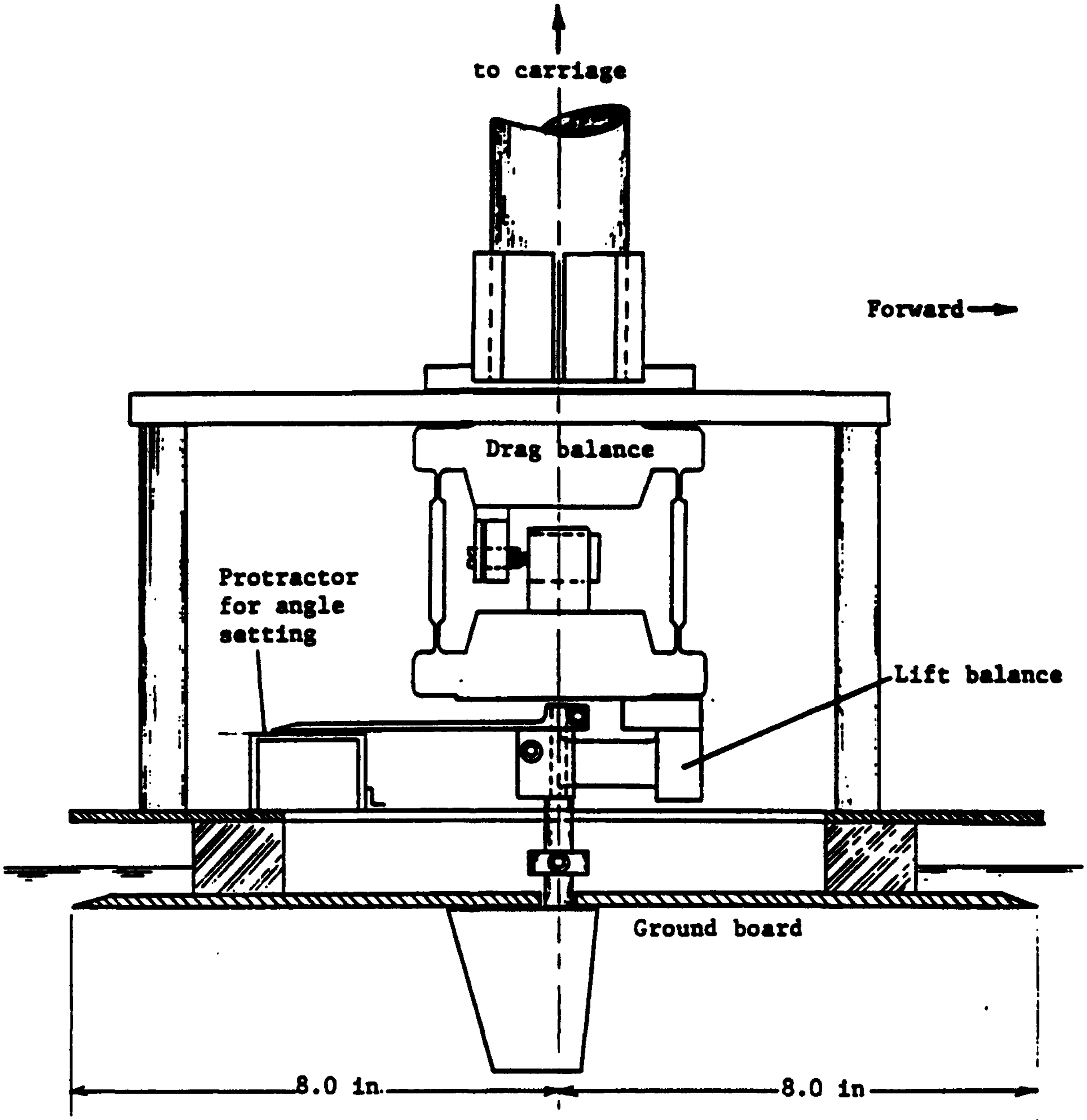

FIGURE 3 APPARATUS FOR MEASURING LIFT AND DRAG OF FINS AGAINST A GROUND BOARD

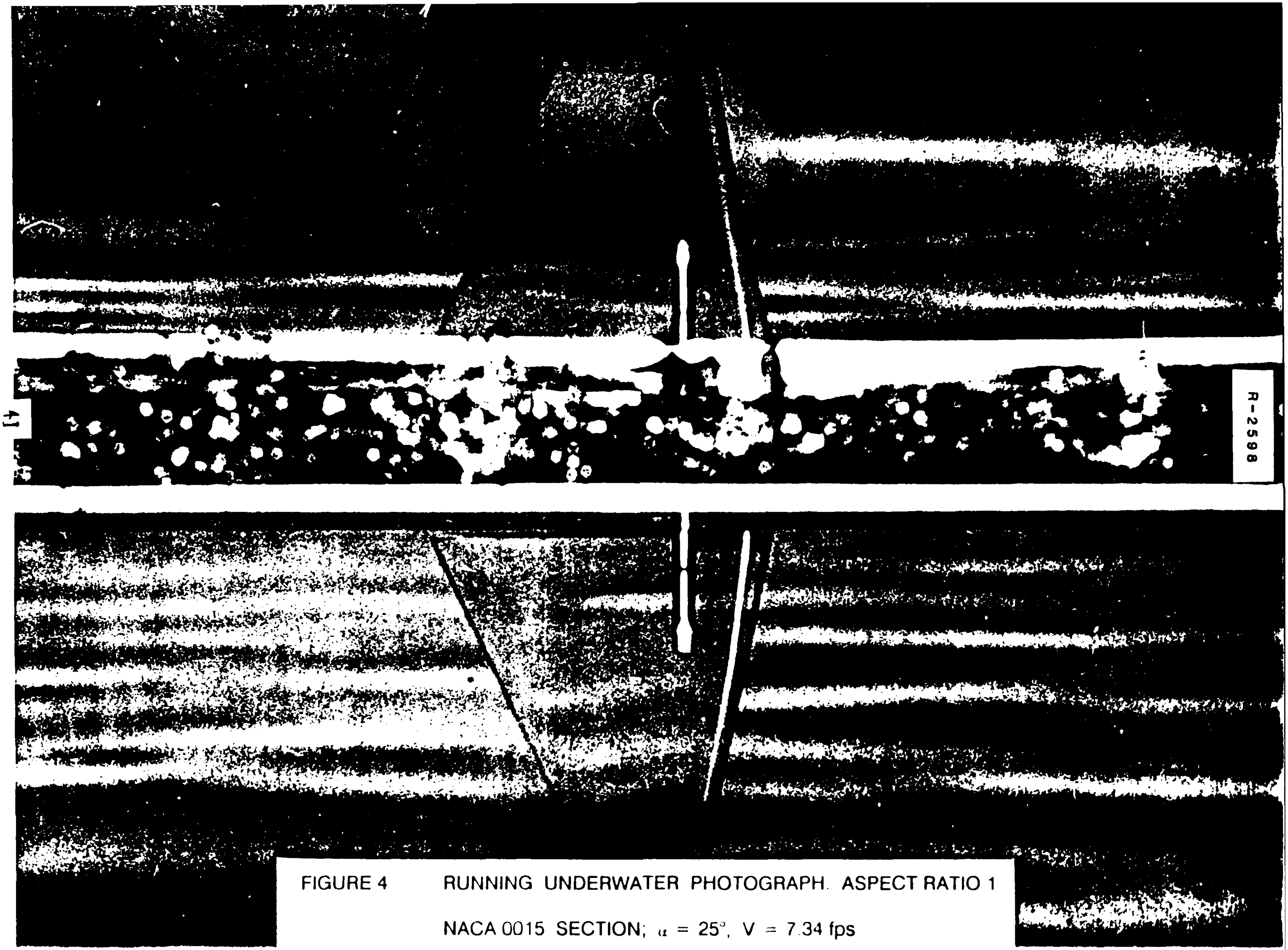

FIGURE 4 RUNNING UNDERWATER PHOTOGRAPH. ASPECT RATIO 1

NACA 0015 SECTION; $\alpha = 25°$, $V = 7.34$ fps

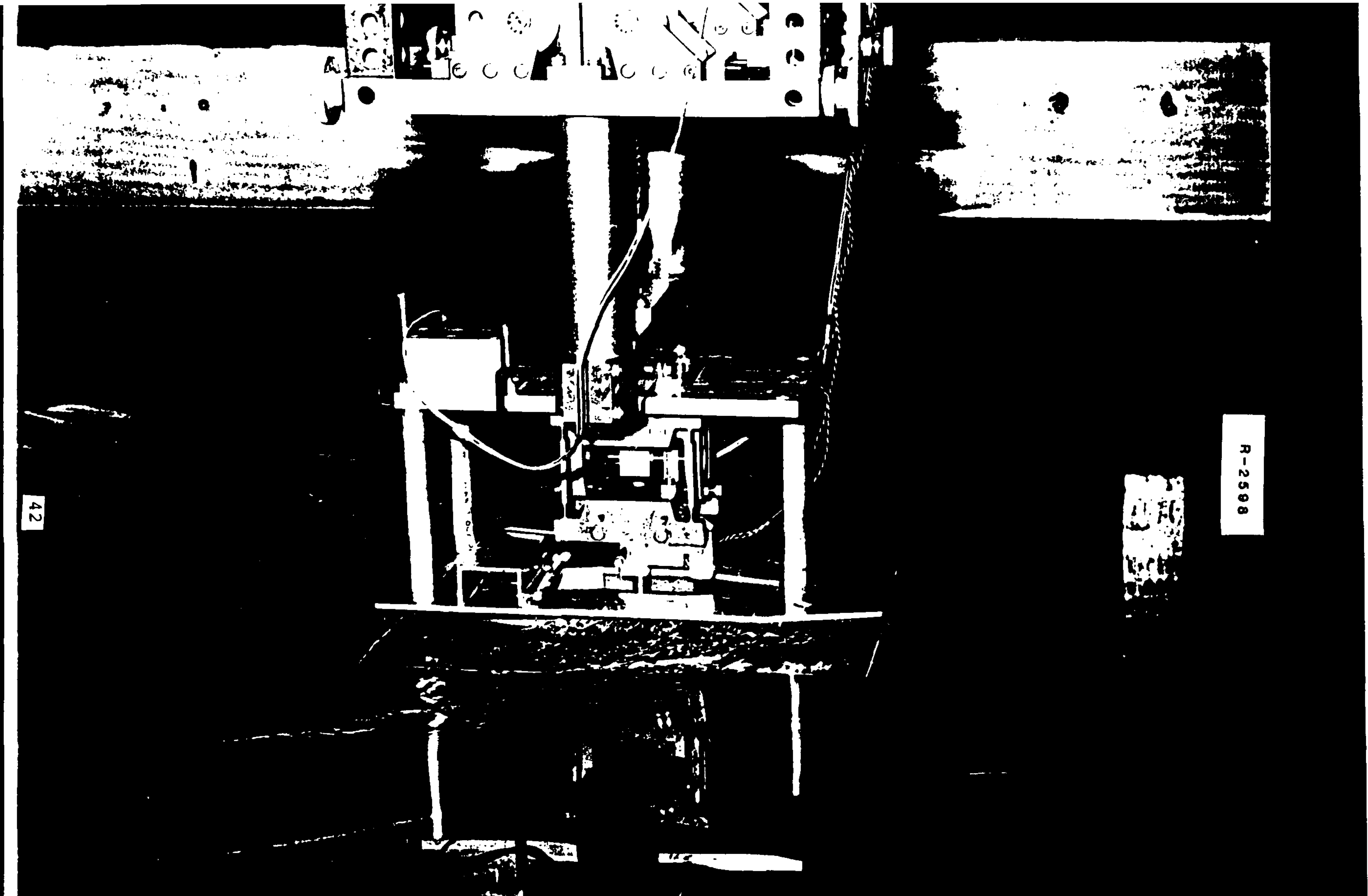

FIGURE 5 RUNNING PHOTOGRAPH OF APPARATUS. V = 7.41 fps

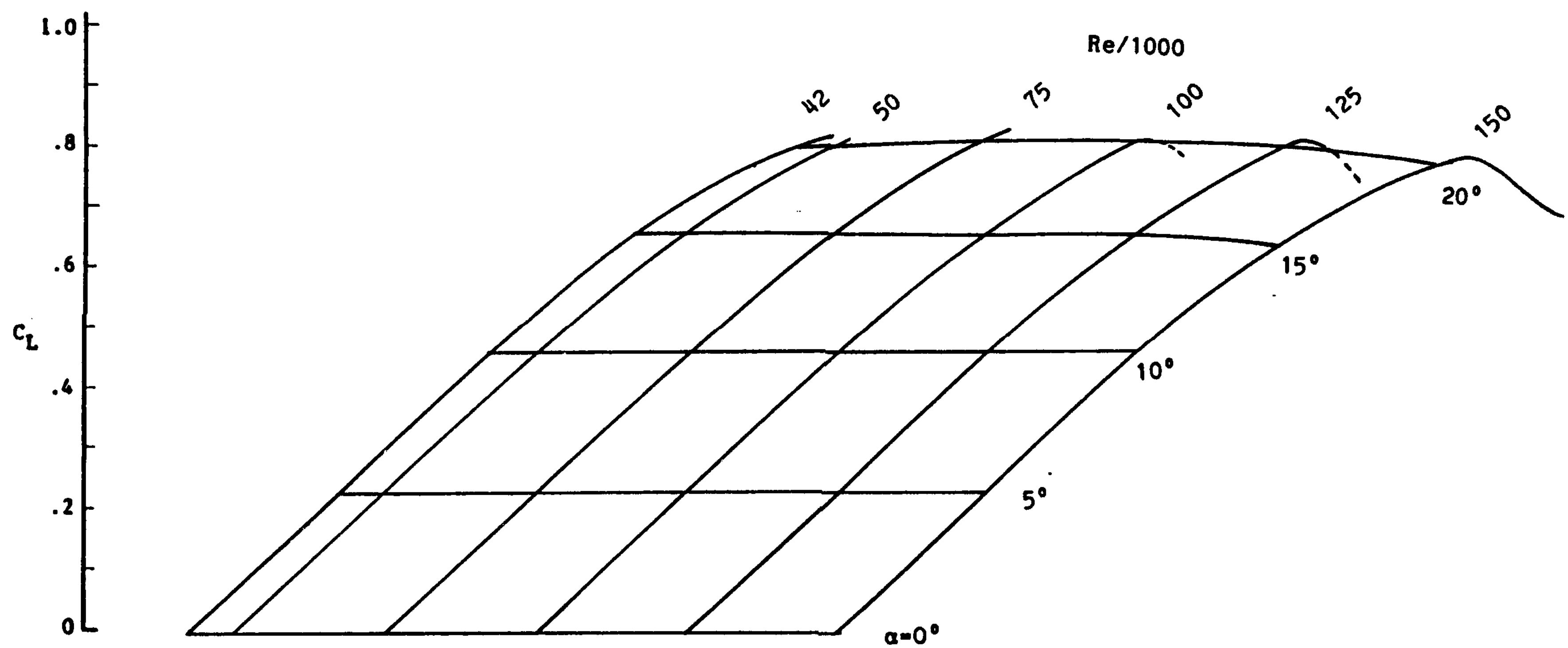

FIGURE 6 LIFT COEFFICIENT OF ASPECT RATIO 1 FLAT PLATE WITHOUT TRIPS.

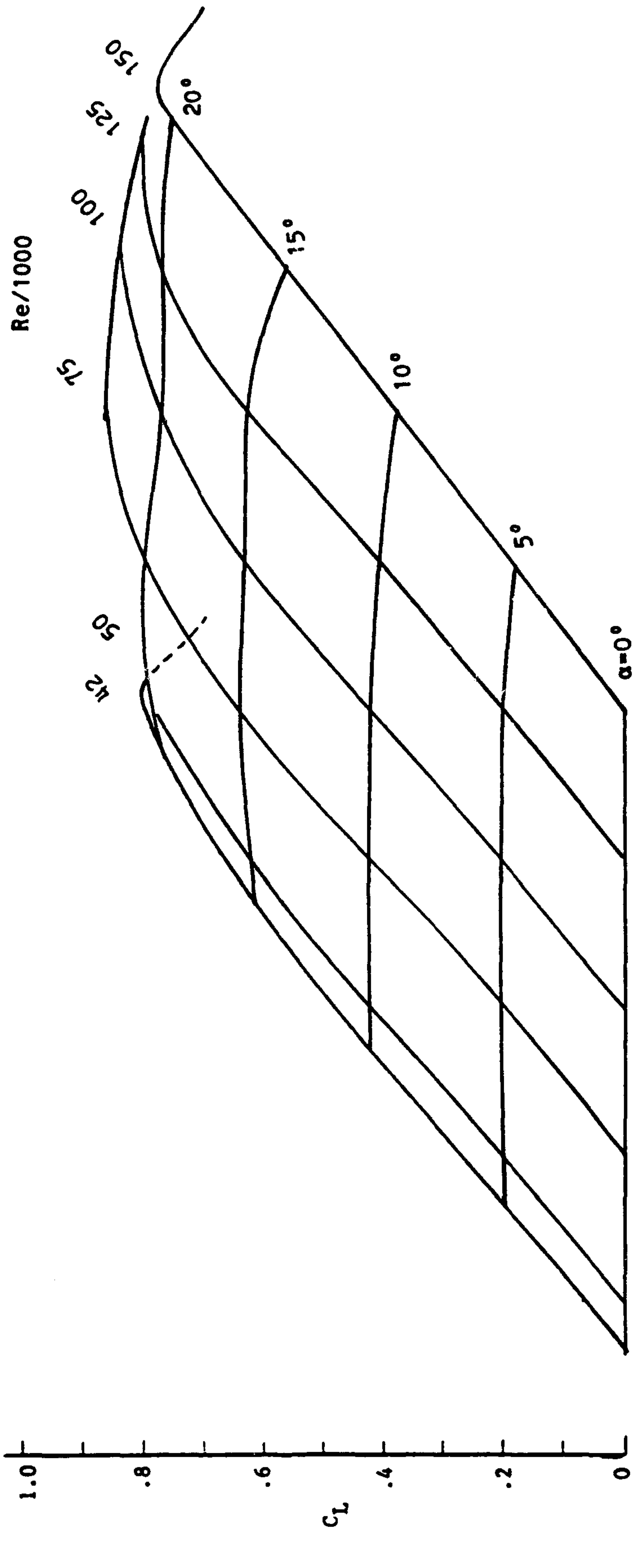

FIGURE 7 LIFT COEFFICIENT OF ASPECT RATIO 1 FLAT PLATE WITH TRIPS.

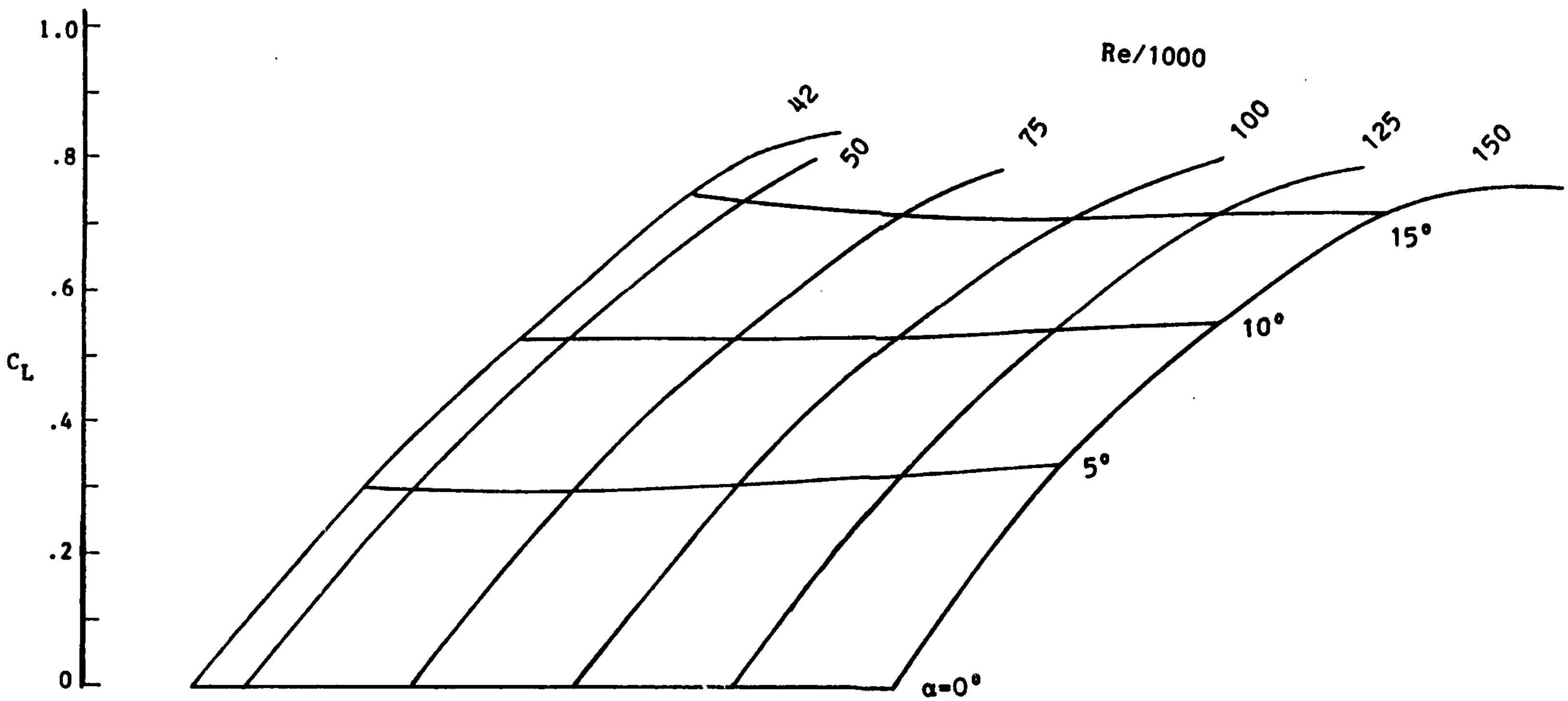

FIGURE 8 LIFT COEFFICIENT OF ASPECT RATIO 1.5 FLAT PLATE WITHOUT TRIPS.

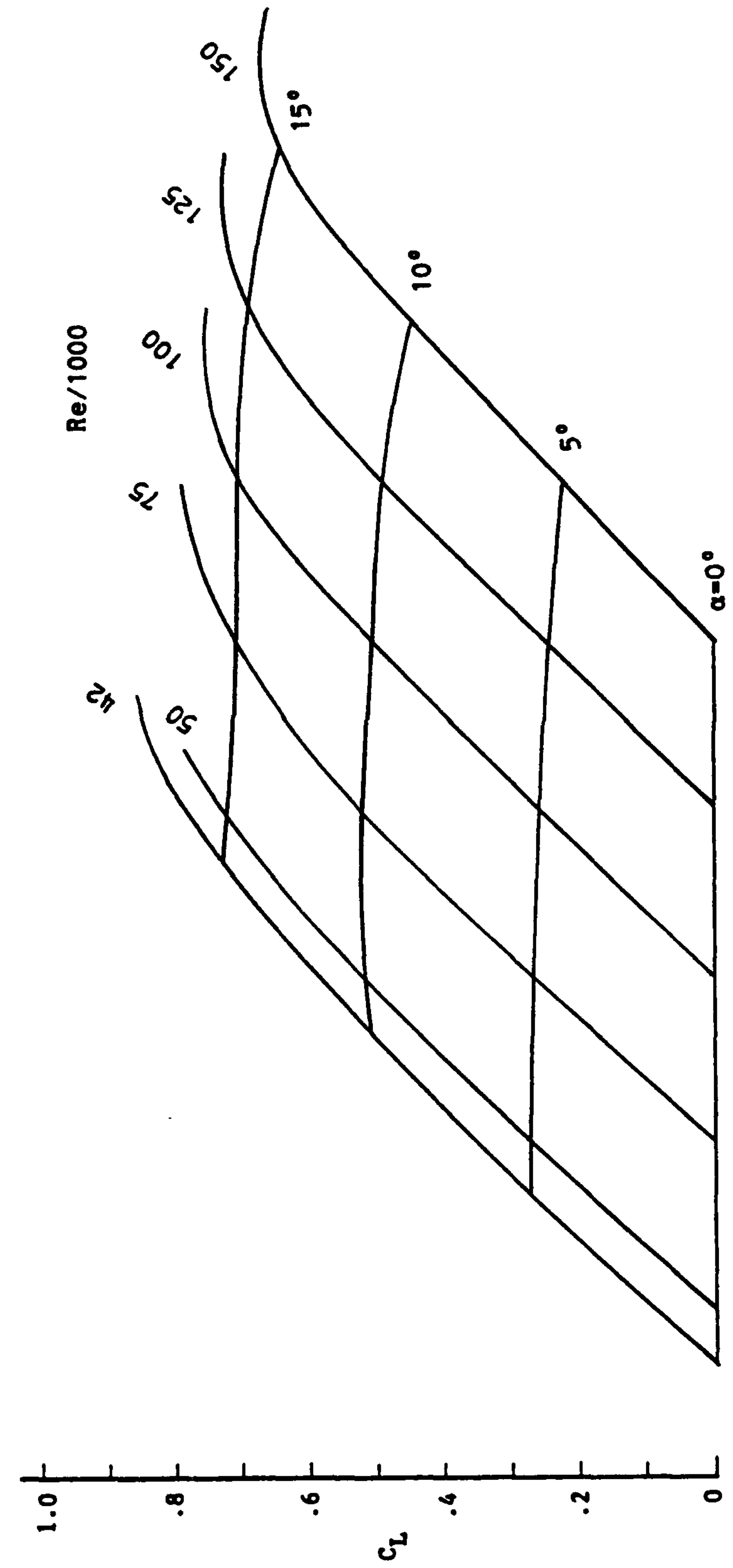

FIGURE 9 LIFT COEFFICIENT OF ASPECT RATIO 1.5 FLAT PLATE WITH TRIPS.

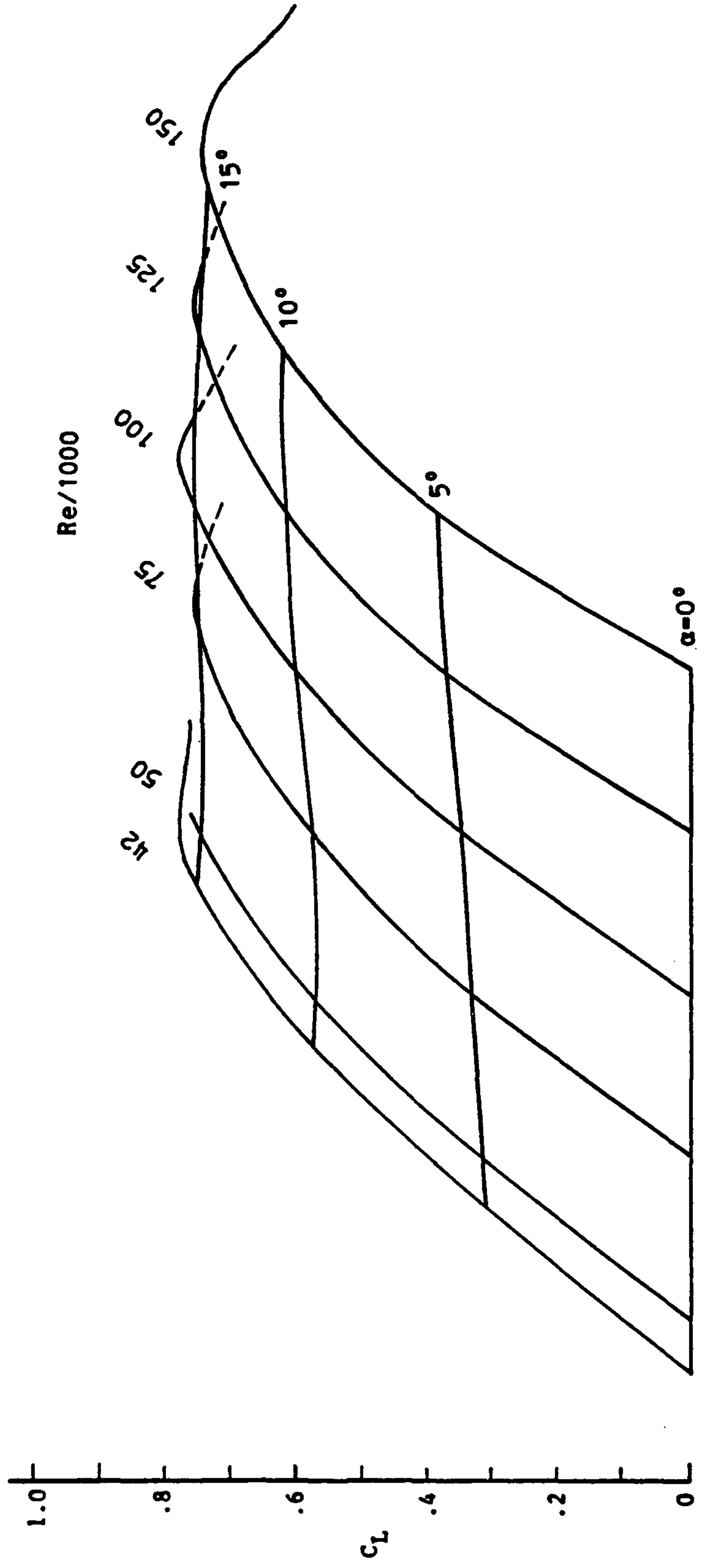

FIGURE 10   LIFT COEFFICIENT OF ASPECT RATIO 2 FLAT PLATE WITHOUT TRIPS.

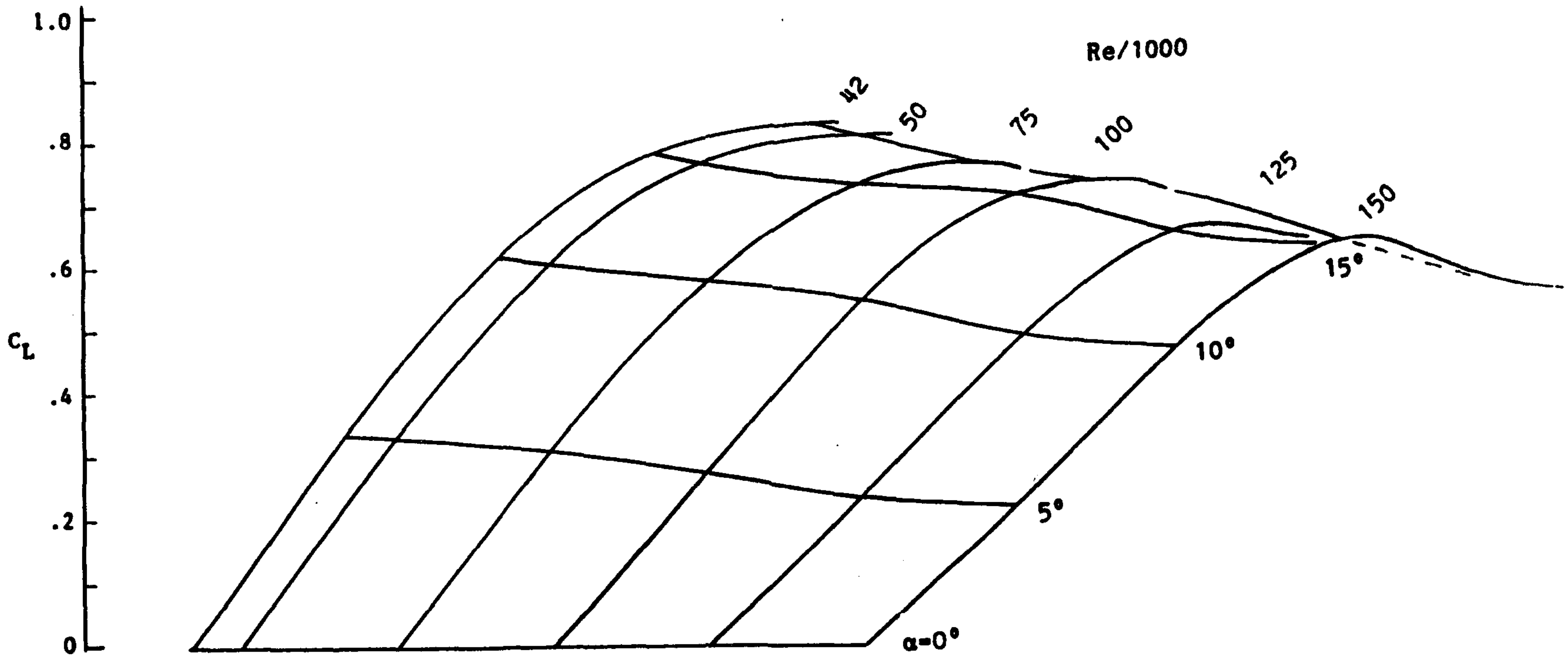

FIGURE 11 LIFT COEFFICIENT OF ASPECT RATIO 2 FLAT PLATE WITH TRIPS.

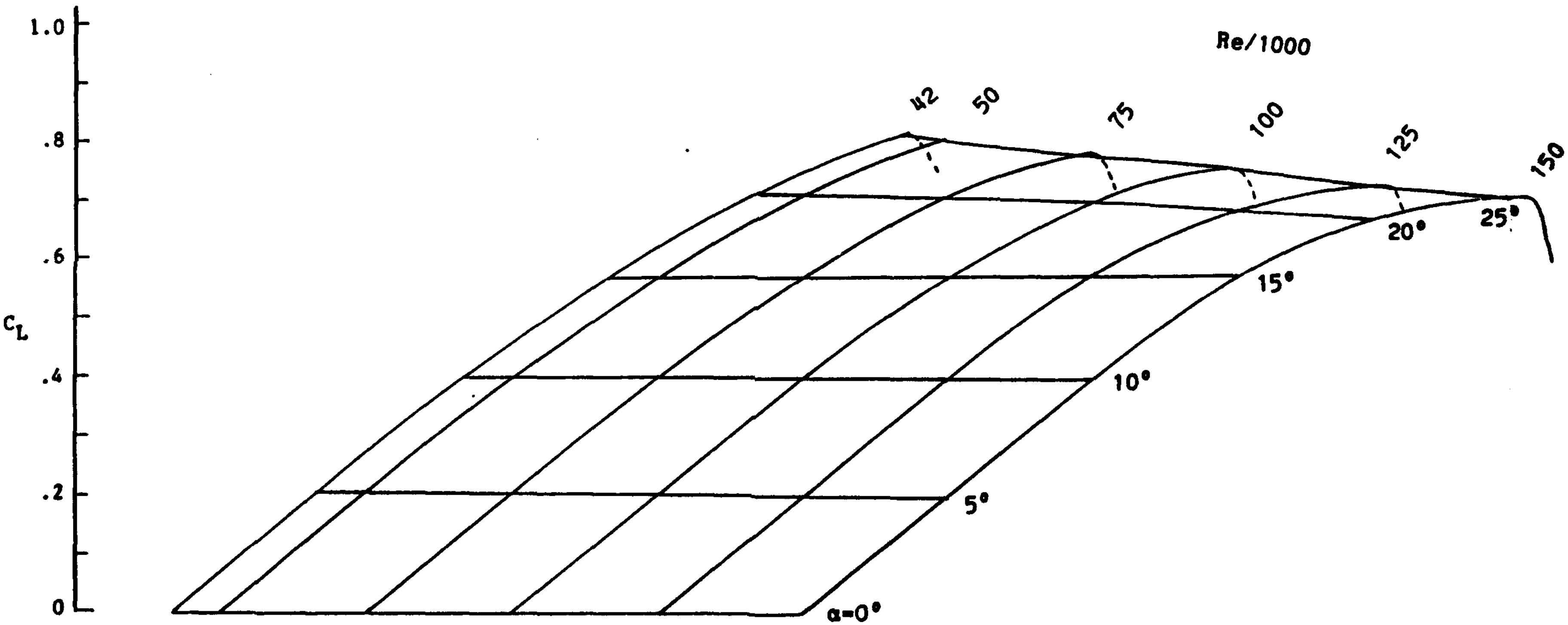

FIGURE 12 LIFT COEFFICIENT OF ASPECT RATIO 1 FIN WITHOUT TRIPS, NACA 0015.

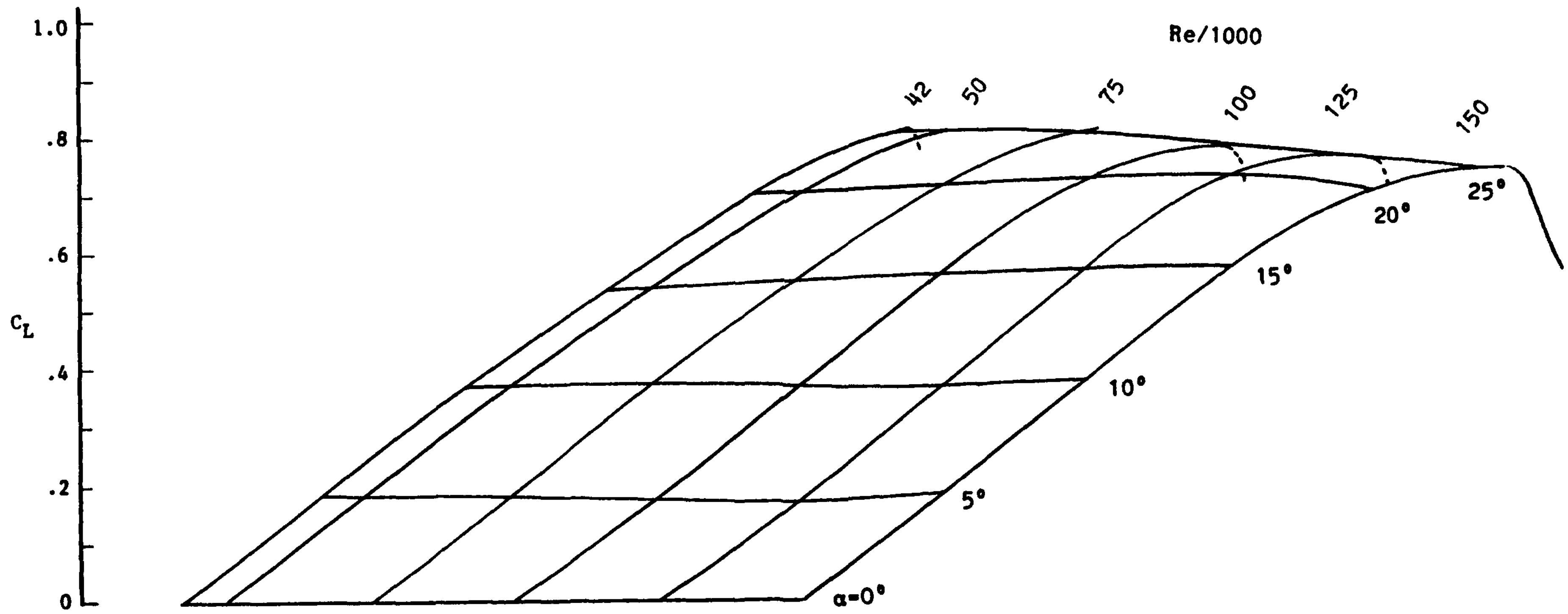

FIGURE 13 LIFT COEFFICIENT OF ASPECT RATIO 1 FIN WITH TRIPS, NACA 0015.

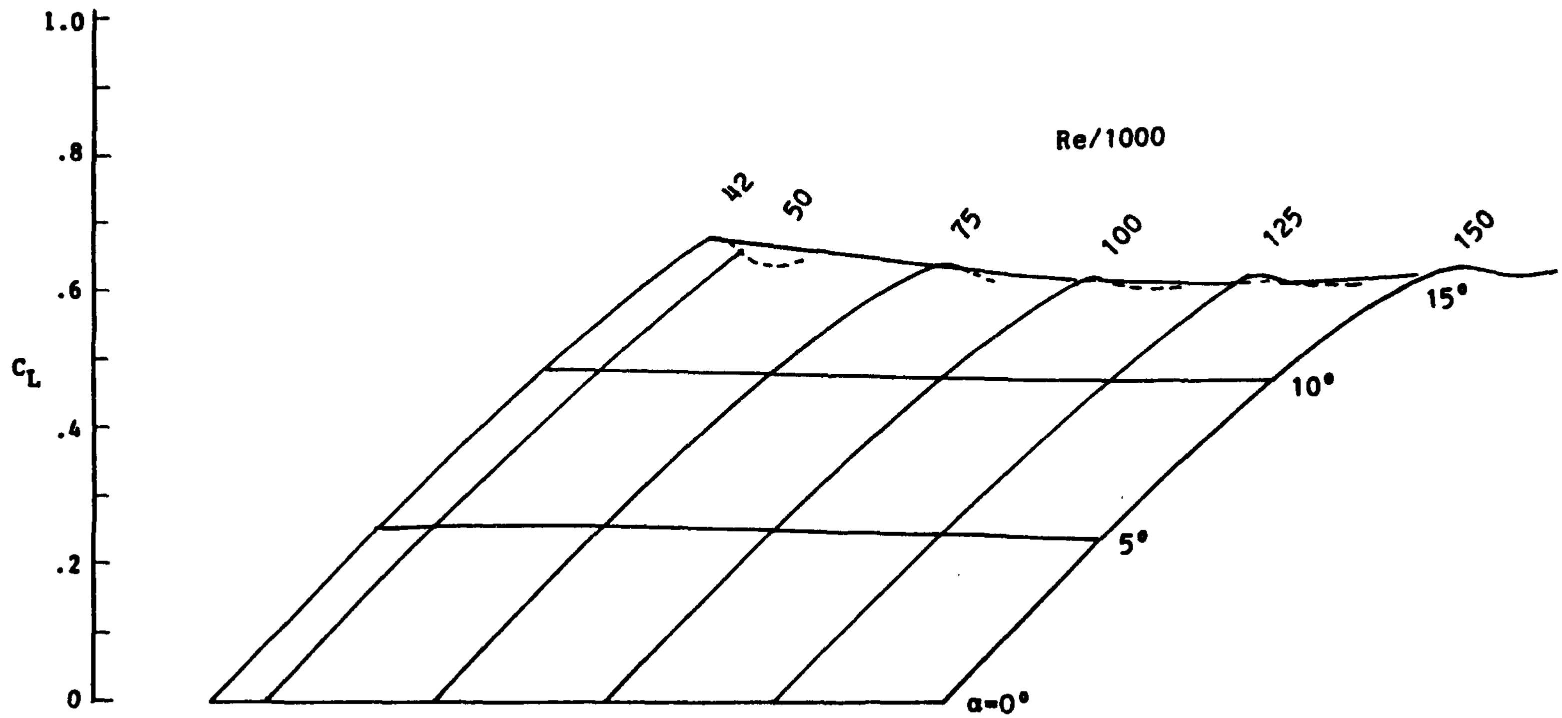

FIGURE 14 LIFT COEFFICIENT FOR ASPECT RATIO 1.5 FIN WITHOUT TRIPS, NACA 0015.

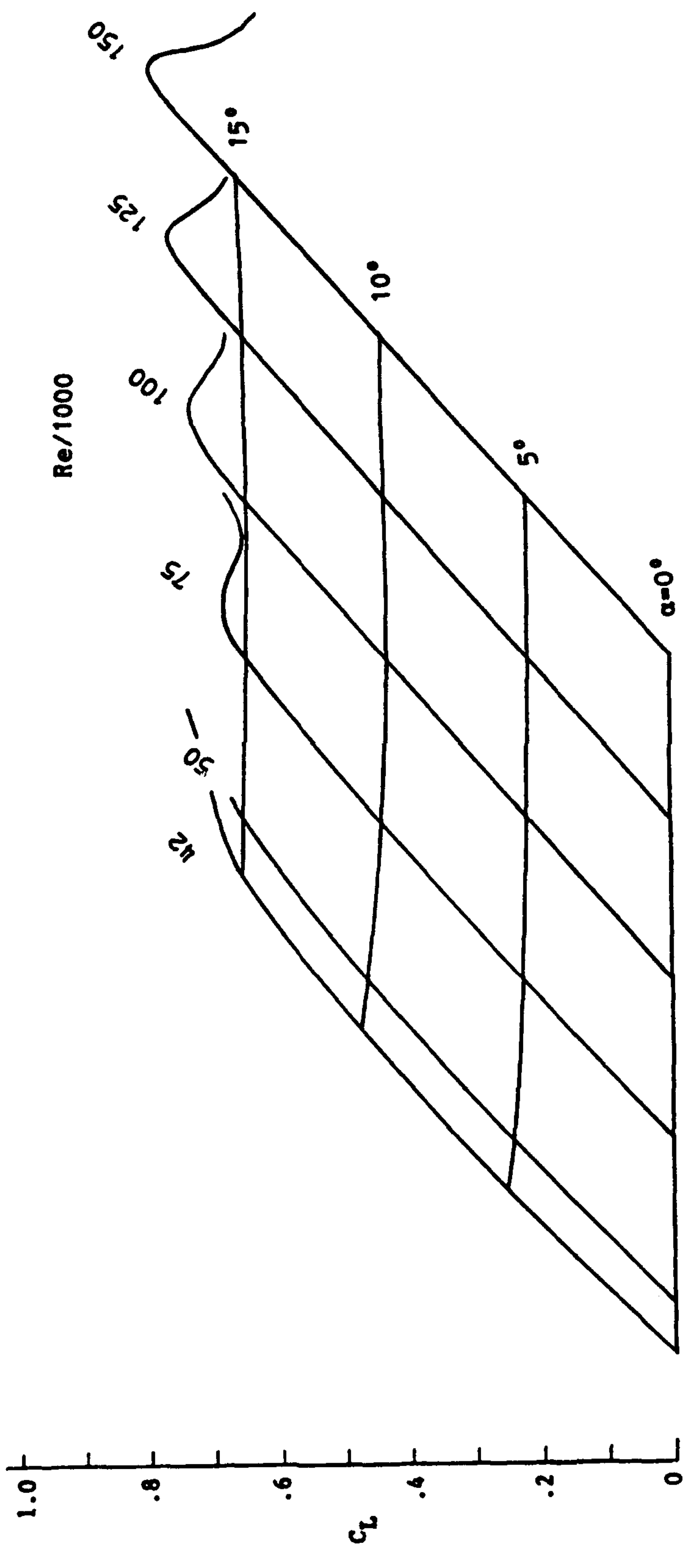

FIGURE 15 LIFT COEFFICIENT FOR ASPECT RATIO 1.5 FIN WITH TRIPS, NACA 0015.

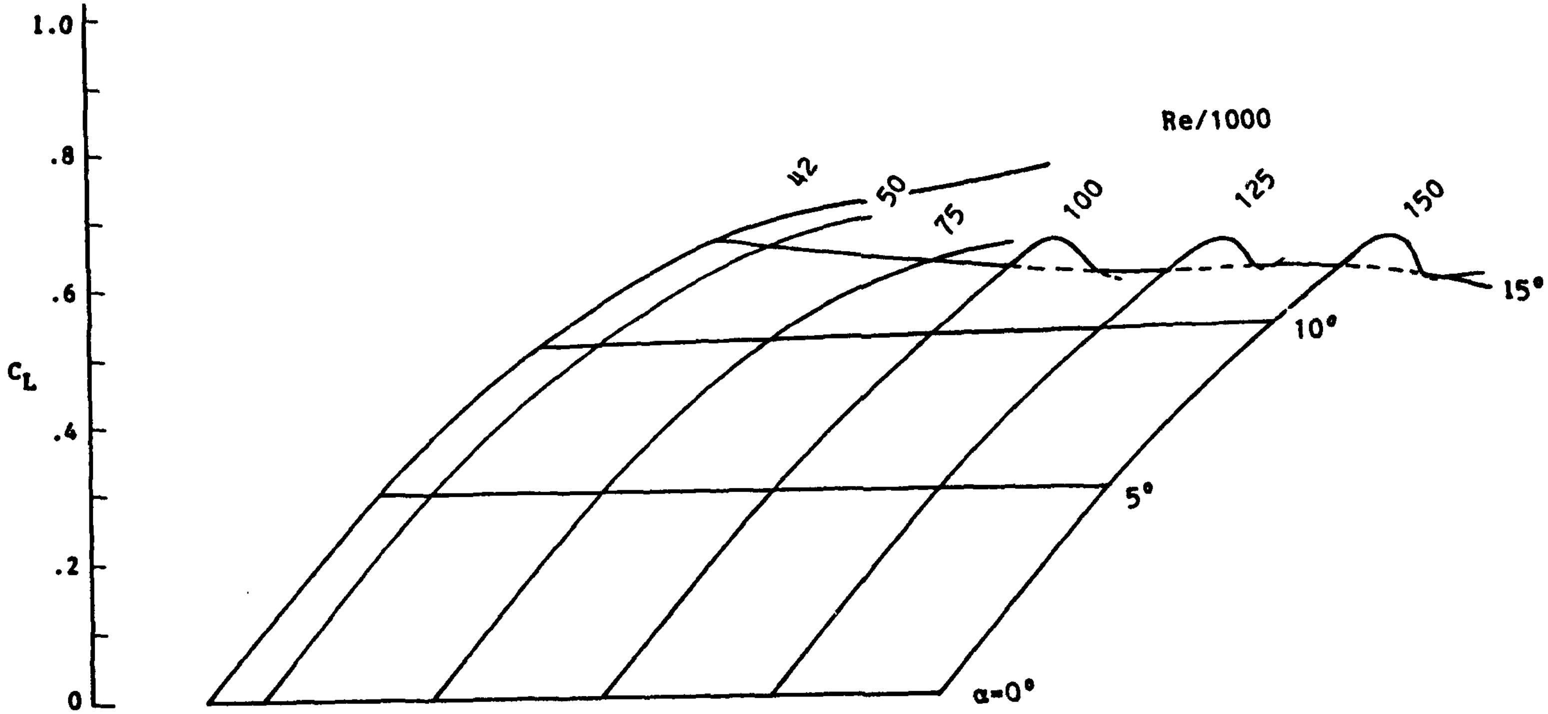

FIGURE 16 LIFT COEFFICIENT FOR ASPECT RATIO 2 FIN WITHOUT TRIPS, NACA 0015.

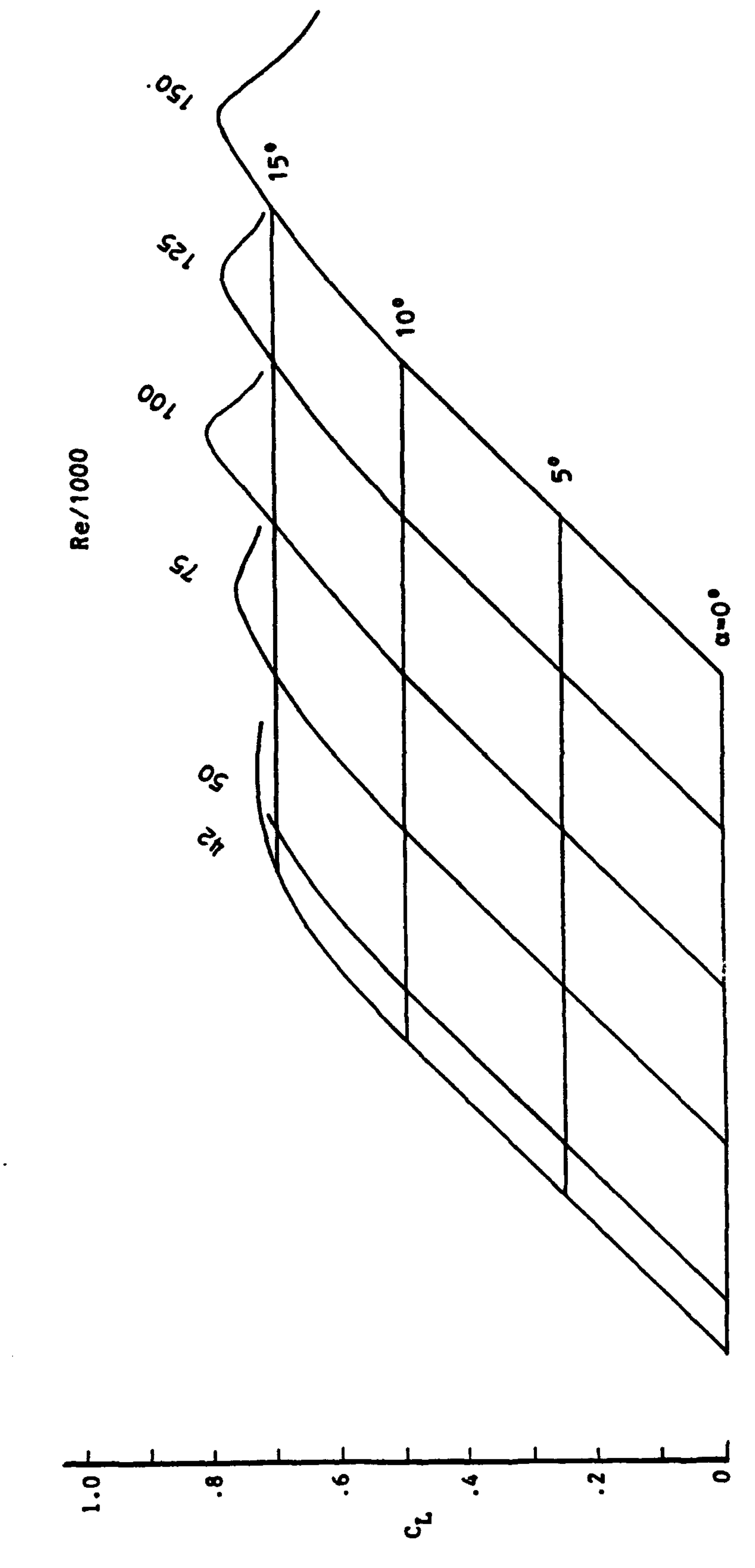

FIGURE 17 LIFT COEFFICIENT FOR ASPECT RATIO 2 FIN WITH TRIPS, NACA 0015.

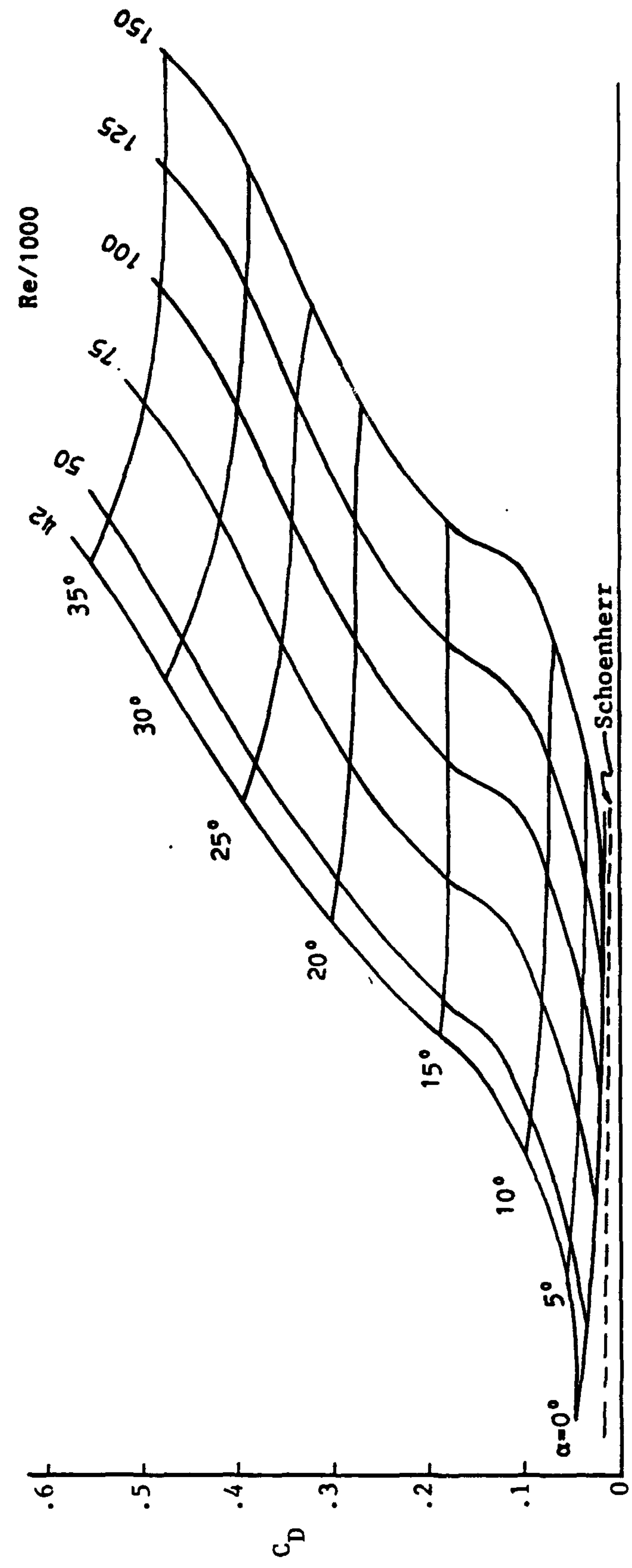

FIGURE 18 DRAG COEFFICIENT OF ASPECT RATIO 2 FIN WITHOUT TRIPS, NACA 0015.

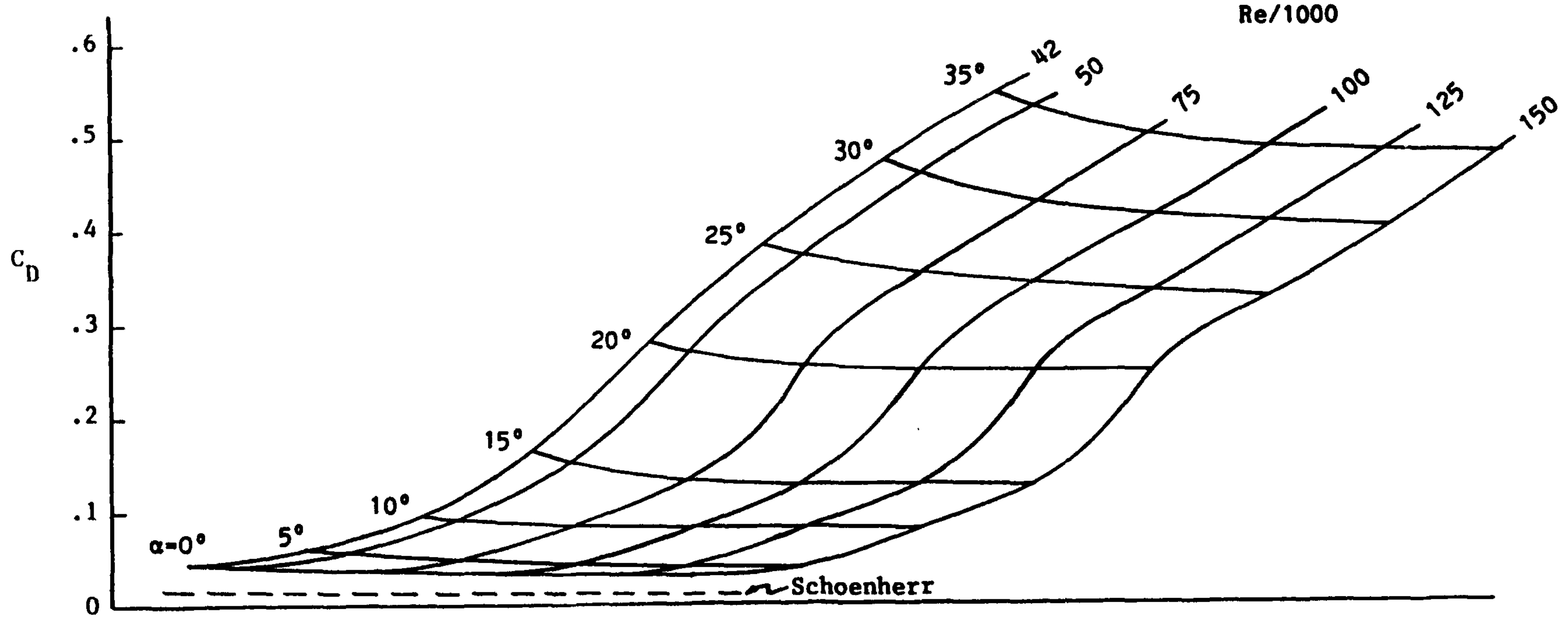

FIGURE 19   DRAG COEFFICIENT OF ASPECT RATIO 2 FIN WITH TRIPS, NACA 0015.

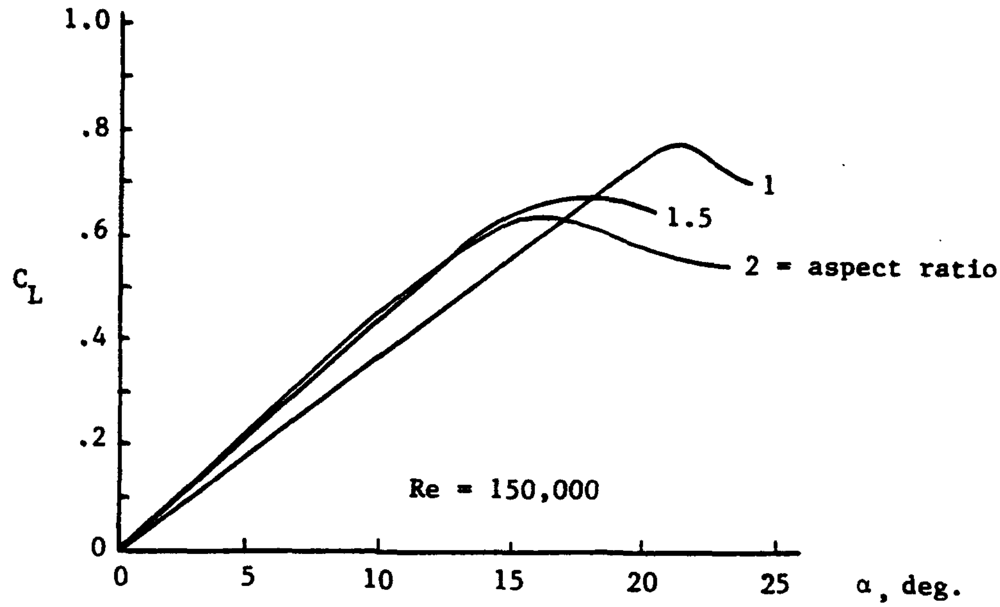

FIGURE 20 EFFECT OF ASPECT RATIO ON LIFT CURVE FOR FLAT PLATE SECTION, WITH TRIPS.

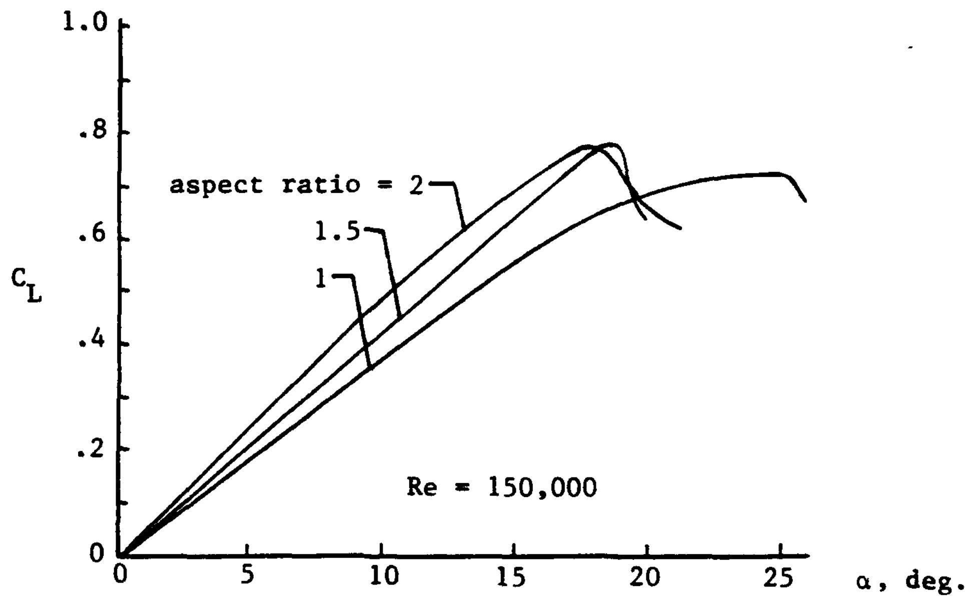

FIGURE 21 EFFECT OF ASPECT RATIO ON LIFT CURVE FOR NACA SECTION, WITH TRIPS.

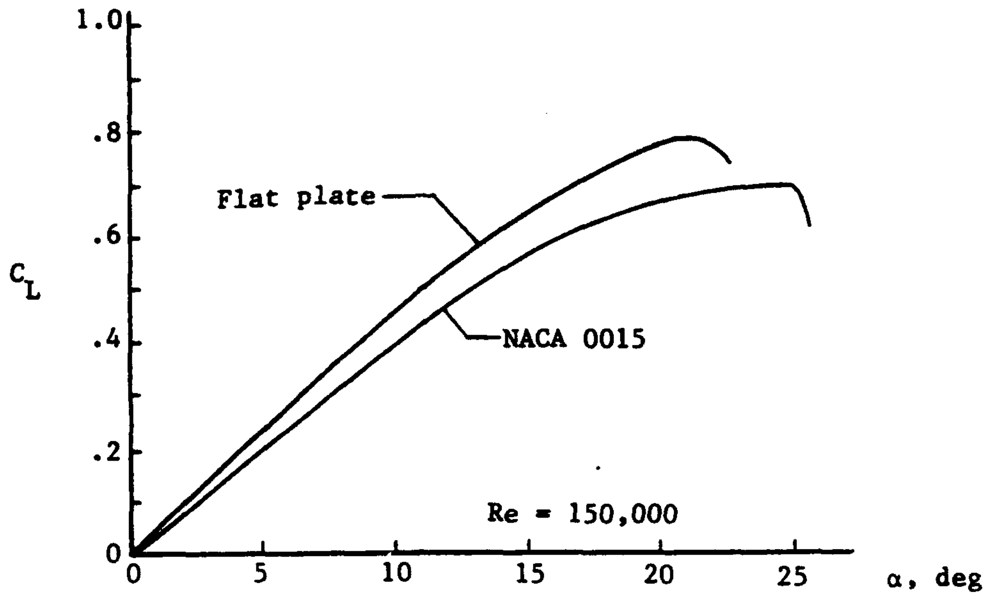

FIGURE 22 EFFECT OF SECTION SHAPE ON LIFT CURVE FOR ASPECT RATIO 1 FINS WITHOUT TRIPS.

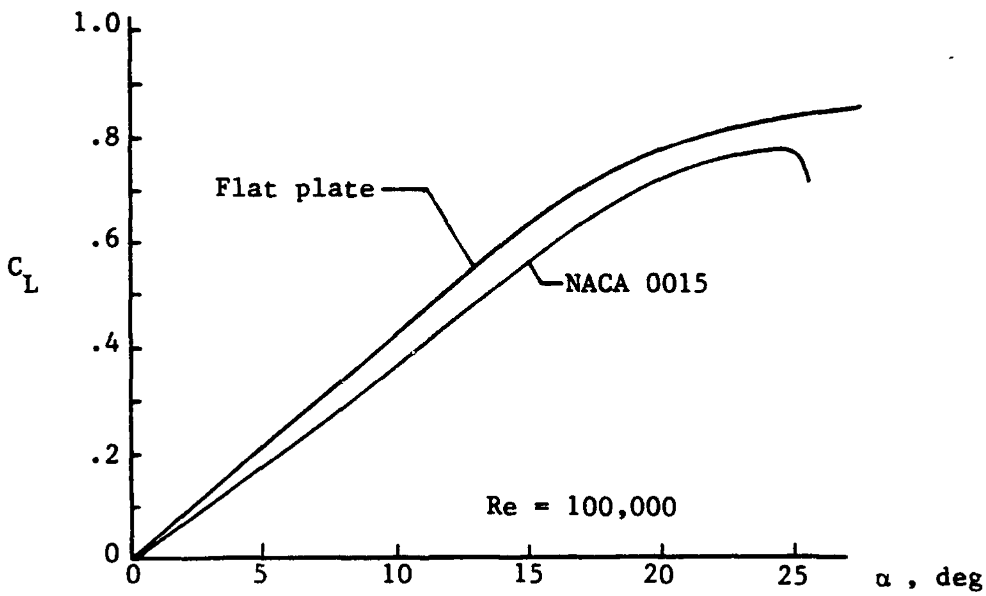

FIGURE 23 EFFECT OF SECTION SHAPE ON LIFT CURVE FOR ASPECT RATIO 1 FINS WITH TRIPS.

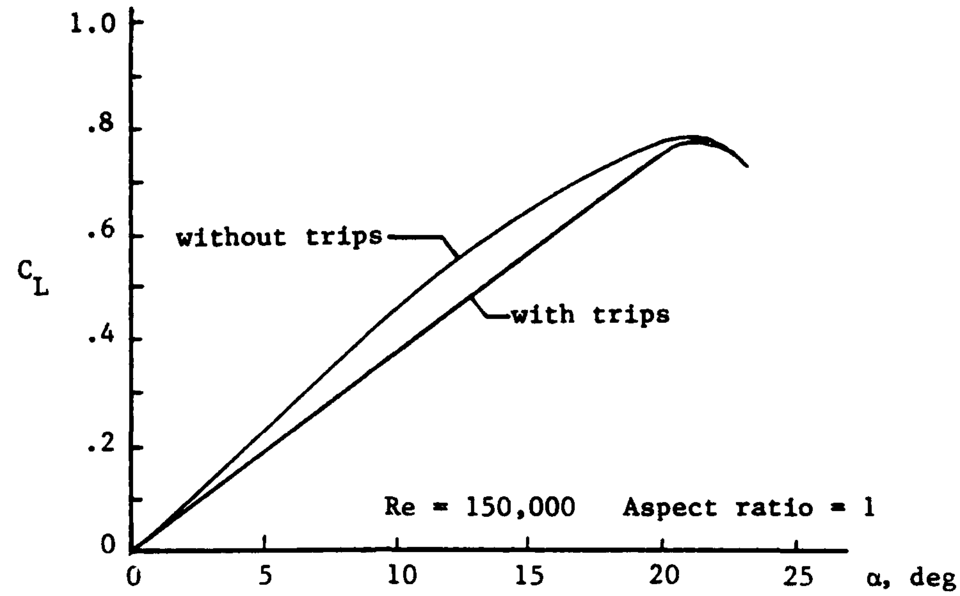

FIGURE 24 EFFECT OF TURBULENCE TRIPS ON LIFT CURVE OF FLAT PLATE FIN.

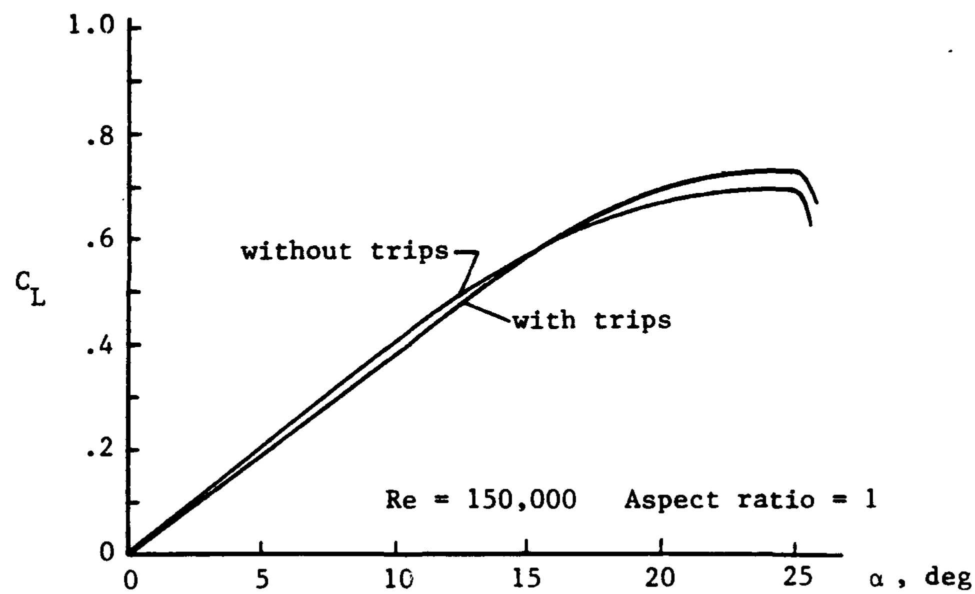

FIGURE 25 EFFECT OF TURBULENCE TRIPS ON LIFT CURVE OF NACA 0015 FIN.

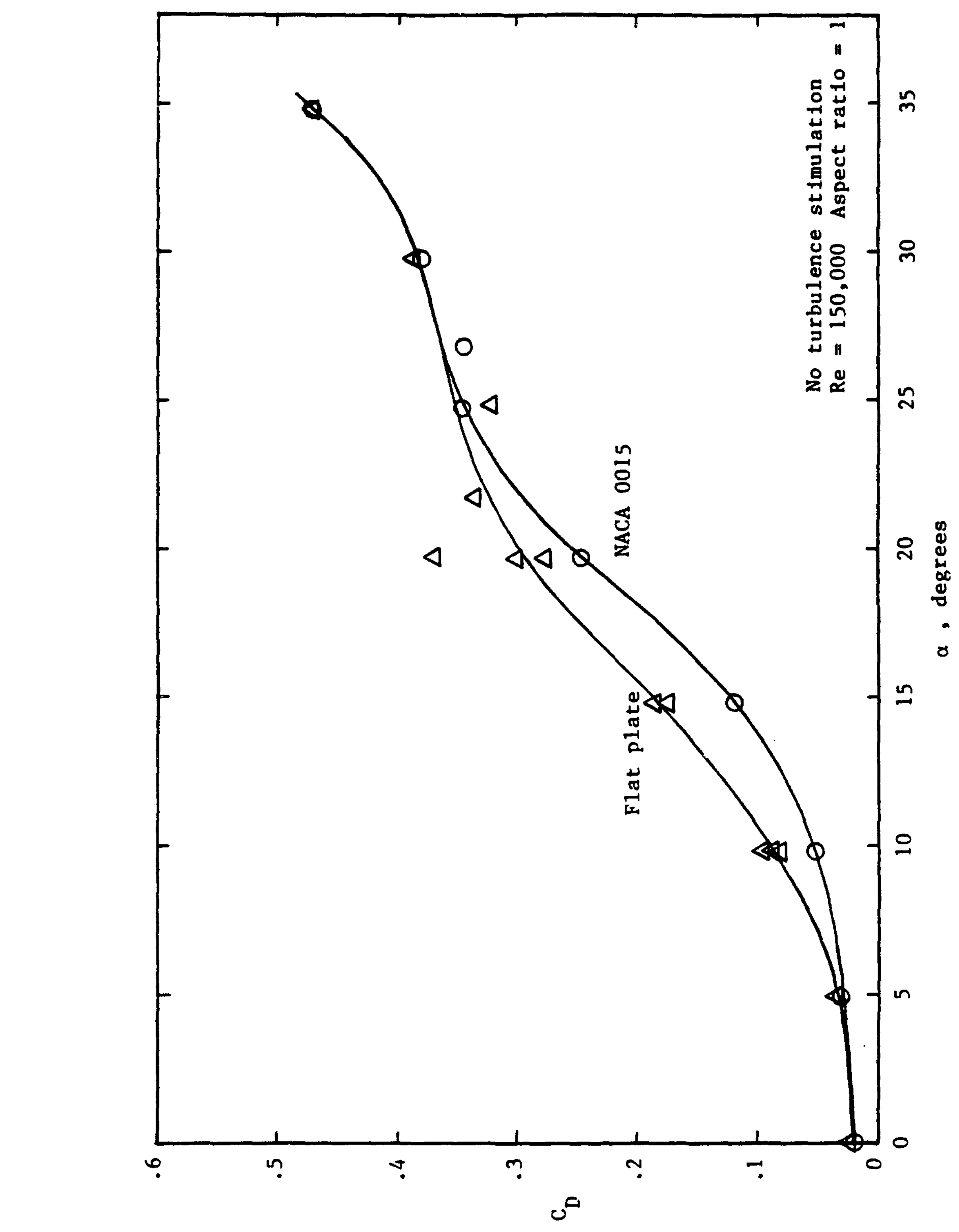

FIGURE 26 EFFECT OF SECTION SHAPE ON DRAG COEFFICIENT

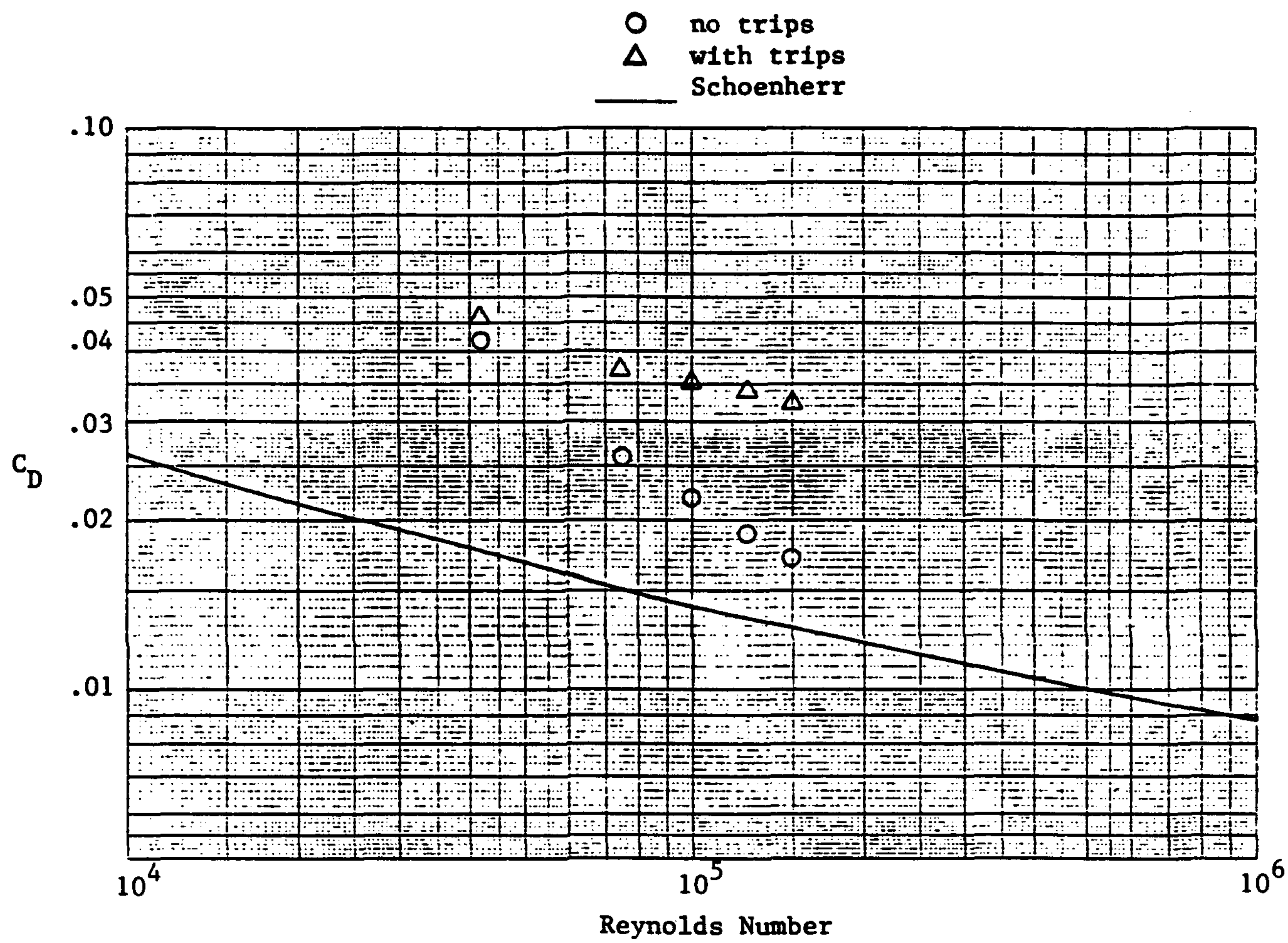

FIGURE 27 DRAG COEFFICIENT OF ASPECT RATIO 2 FIN (NACA 0015) AT $\alpha = 0°$

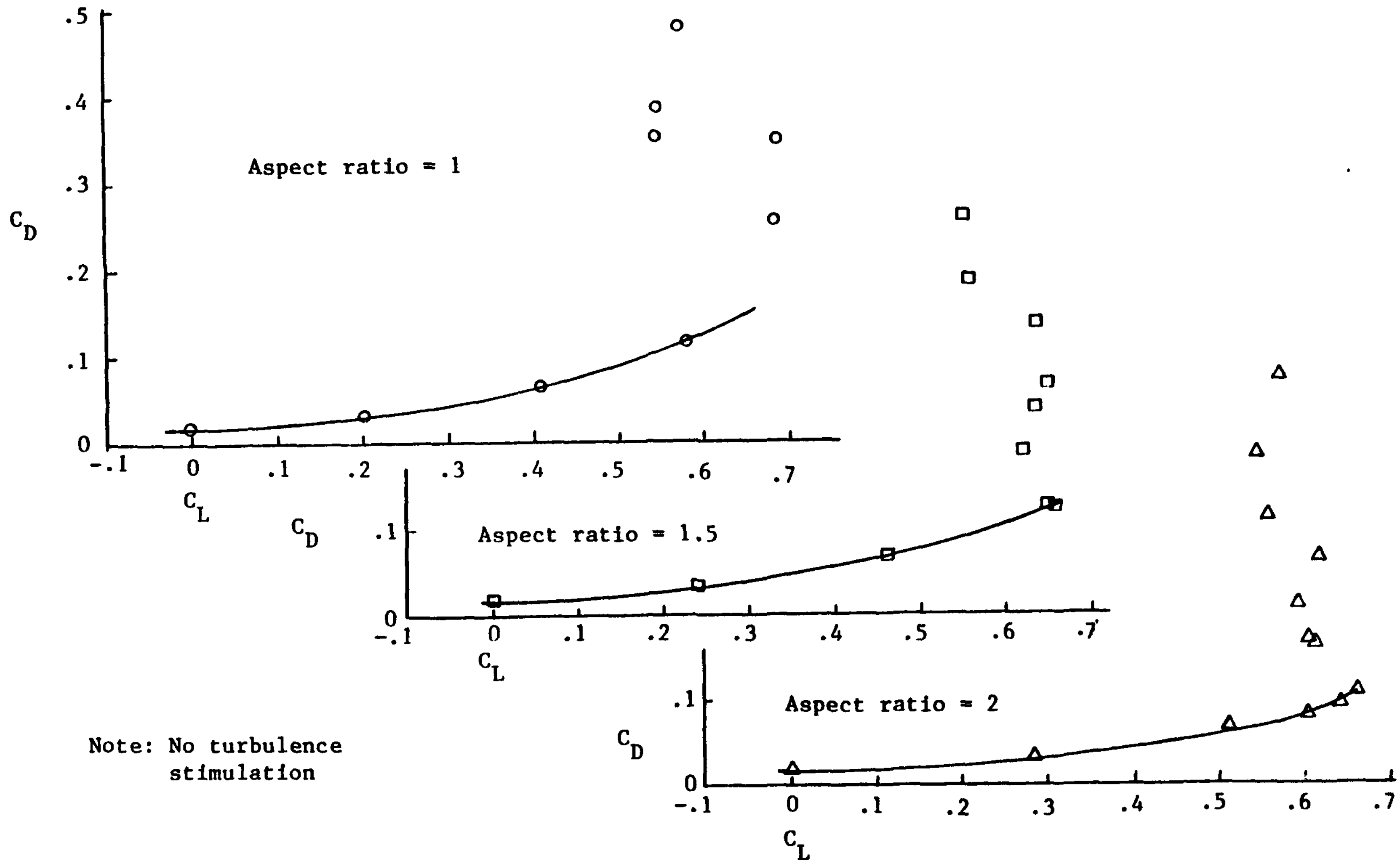

FIGURE 28 DRAG POLARS FOR NACA 0015 FIN AT Re = 150,000

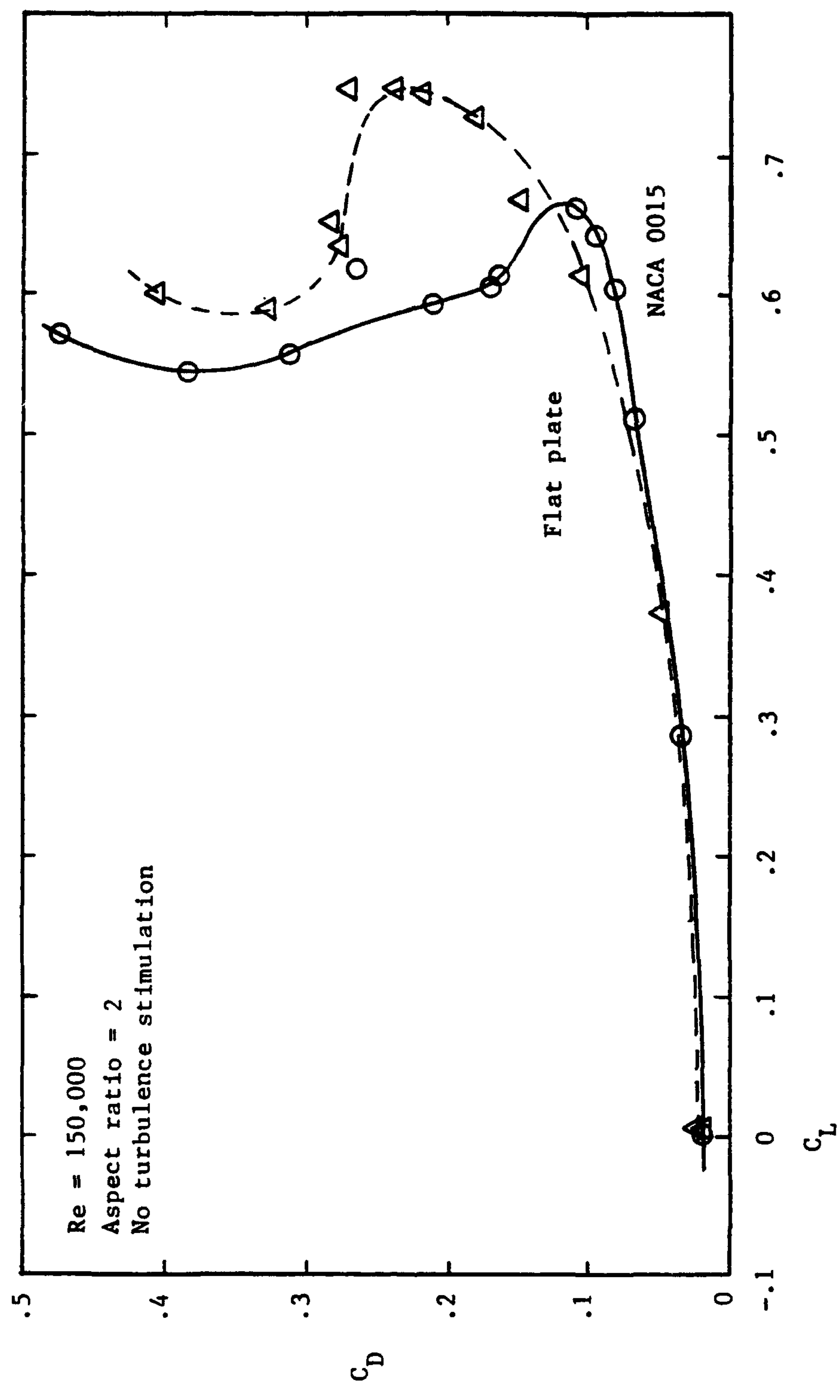

FIGURE 29 EFFECT OF SECTION SHAPE ON DRAG POLAR

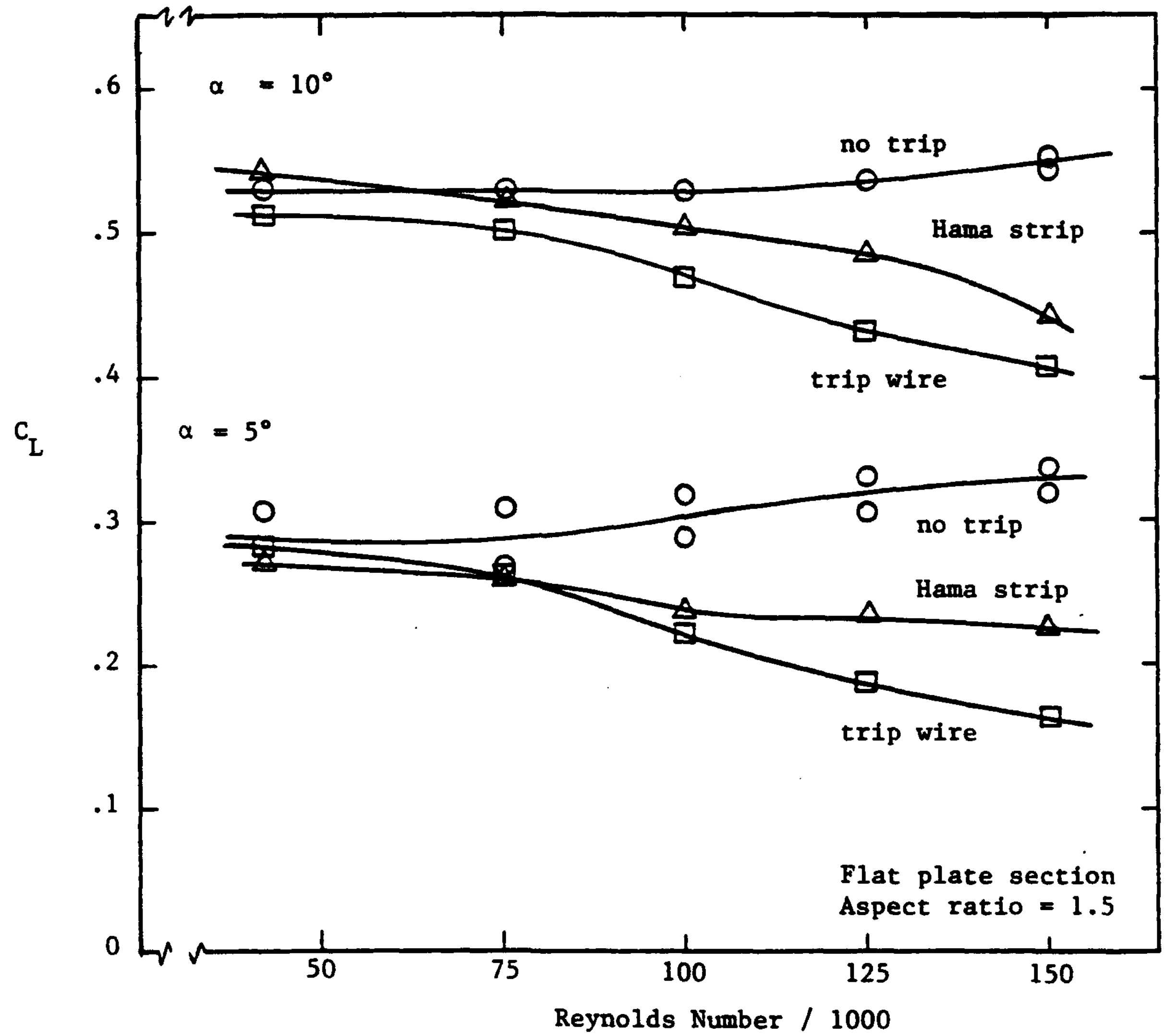

FIGURE 30 EFFECT OF TURBULENCE STIMULATORS AND REYNOLDS NUMBER ON LIFT COEFFICIENT OF FLAT PLATE FIN.

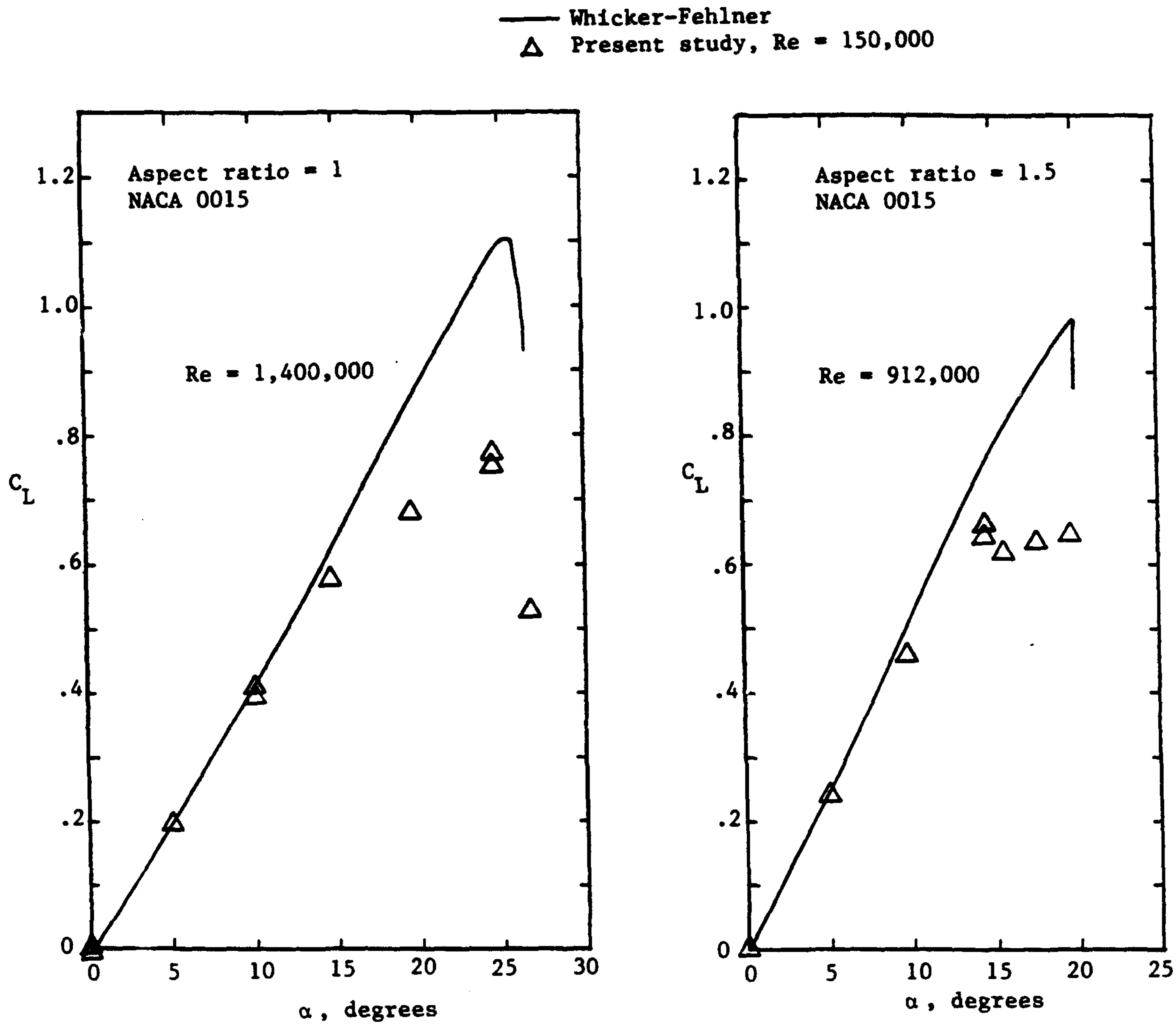

FIGURE 31 COMPARISON OF MEASURED LIFT COEFFICIENTS WITH DATA OF WHICKER AND FEHLNER[6]

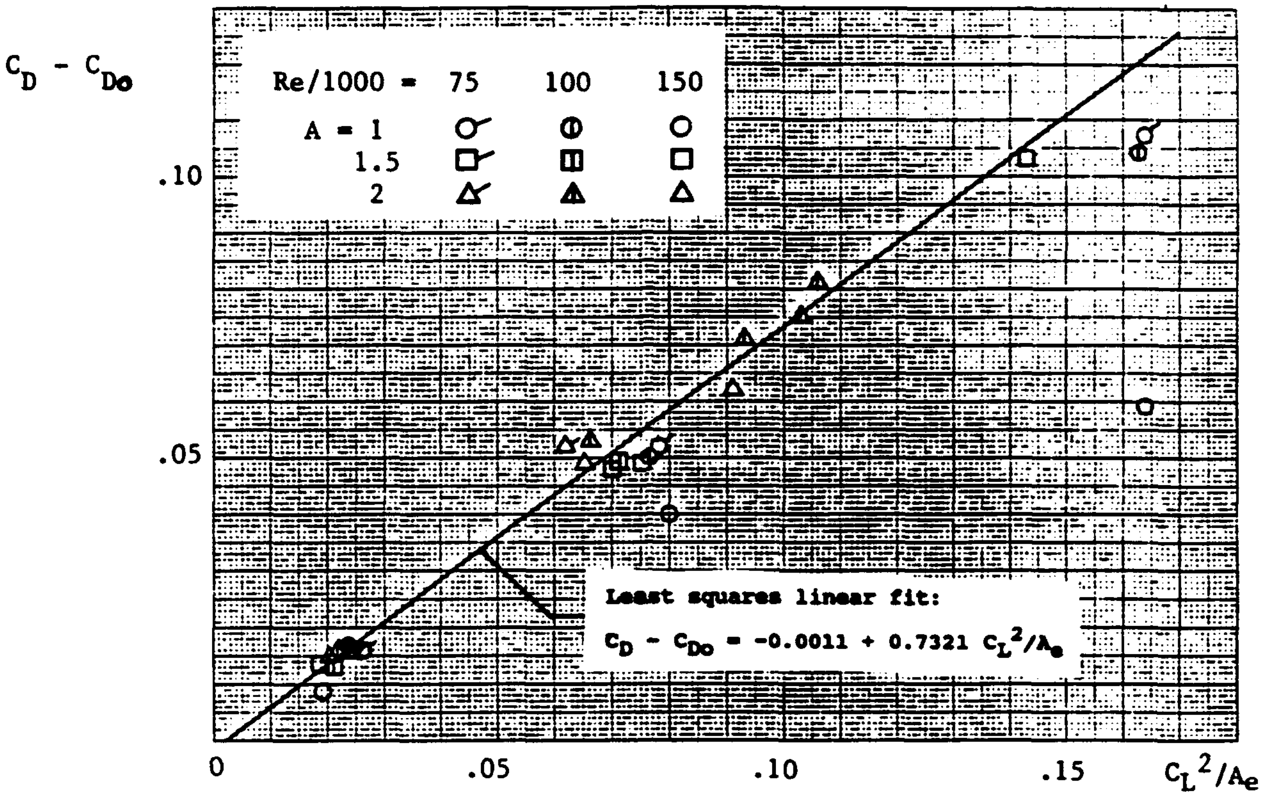

FIGURE 32 PLOT FOR DETERMINATION OF INDUCED DRAG FACTOR

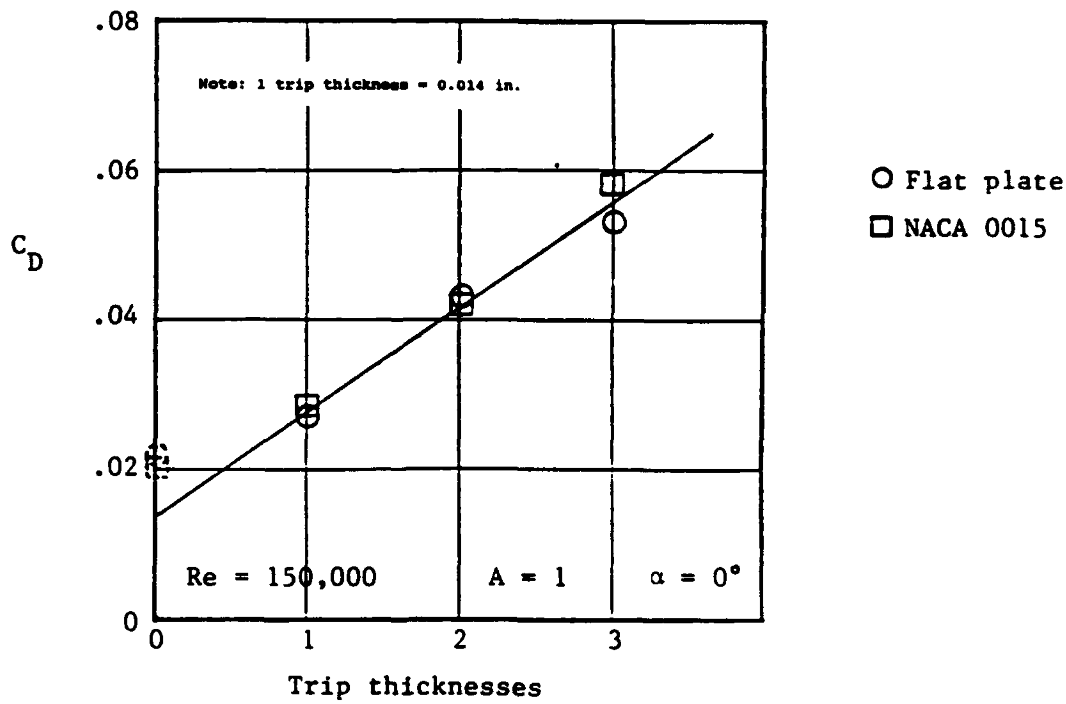

FIGURE 33 EFFECT OF TRIP THICKNESS ON DRAG COEFFICIENT

APPENDIX A
LIFT AND DRAG BALANCE CALIBRATION

The balance was calibrated on a tankside calibration stand, shown in the photograph (Figure A1), by application of known weights at the approximate center of pressure location of the fins to be tested. The apparatus was rotated so that lift, drag, and combinations thereof could be applied. The digitized voltage readings were expressed as linear functions of both lift and drag:

$$\begin{Bmatrix} V_1 \\ V_2 \end{Bmatrix} = \begin{bmatrix} C \end{bmatrix} \begin{Bmatrix} L \\ D \end{Bmatrix}$$

The coefficients in the matrix [C] were determined by means of a multivariate least squares fit. Inversion of this matrix gives the *calibration rates* R_{ij}:

$$\begin{Bmatrix} L \\ D \end{Bmatrix} = \begin{bmatrix} R \end{bmatrix} \begin{Bmatrix} V_1 \\ V_2 \end{Bmatrix} \quad ; \quad \begin{bmatrix} R \end{bmatrix} = \begin{bmatrix} C \end{bmatrix}^{-1} ,$$

where the off-diagonal elements R_{12}, R_{21} represent cross-coupling.

Results of the calibration are summarized below.

Lift Applied	Lift Calculated	Difference	Drag Applied	Drag Calculated	Difference
0.000	0.000	0	0.100	0.100	0
0.000	0.001	0.001	0.200	0.199	-0.001
0.000	0.000	0	0.500	0.501	0.001
0.000	0.000	0	0.700	0.700	0
0.000	0.000	0	1.000	1.001	0.001
0.000	-0.003	-0.003	1.200	1.201	0.001
1.000	1.003	0.003	0.000	0.001	0.001
2.000	2.002	0.002	0.000	0.002	0.002
3.000	2.993	-0.007	0.000	0.002	0.002
0.490	0.490	0.000	0.090	0.087	-0.003
0.980	0.982	0.002	0.170	0.175	0.005
1.970	1.975	0.005	0.350	0.348	-0.002
2.990	2.993	0.003	0.260	0.262	0.002
4.980	4.981	0.001	0.440	0.434	-0.006

The calibration rates are:

$$\text{Lift} = -0.0066923\ V_1 + 0.0000220\ V_2$$
$$\text{Drag} = -0.0000303\ V_1 + 0.0008012\ V_2$$

where V_1 and V_2 are the digitized voltage readings from the lift and drag channels, respectively. The calibration is plotted on Figure A2.

The small deflections in the balance springs under load produced on a small angular deflection of the fins, tending to reduce the angle of attack. A calibration was carried out for angular deflection against lift force, with the following result:

Lift Applied	Angle Measured	Angle Calculated	Difference
0	0	0.00	0
0.50	-0.09	-0.08	0.01
1.00	-0.16	-0.16	0
2.00	-0.30	-0.32	-0.02
3.00	-0.47	-0.48	-0.01
4.00	-0.66	-0.64	0.02

The angular deflection is related to the lift as follows:

$$\Delta\alpha = -0.161L$$

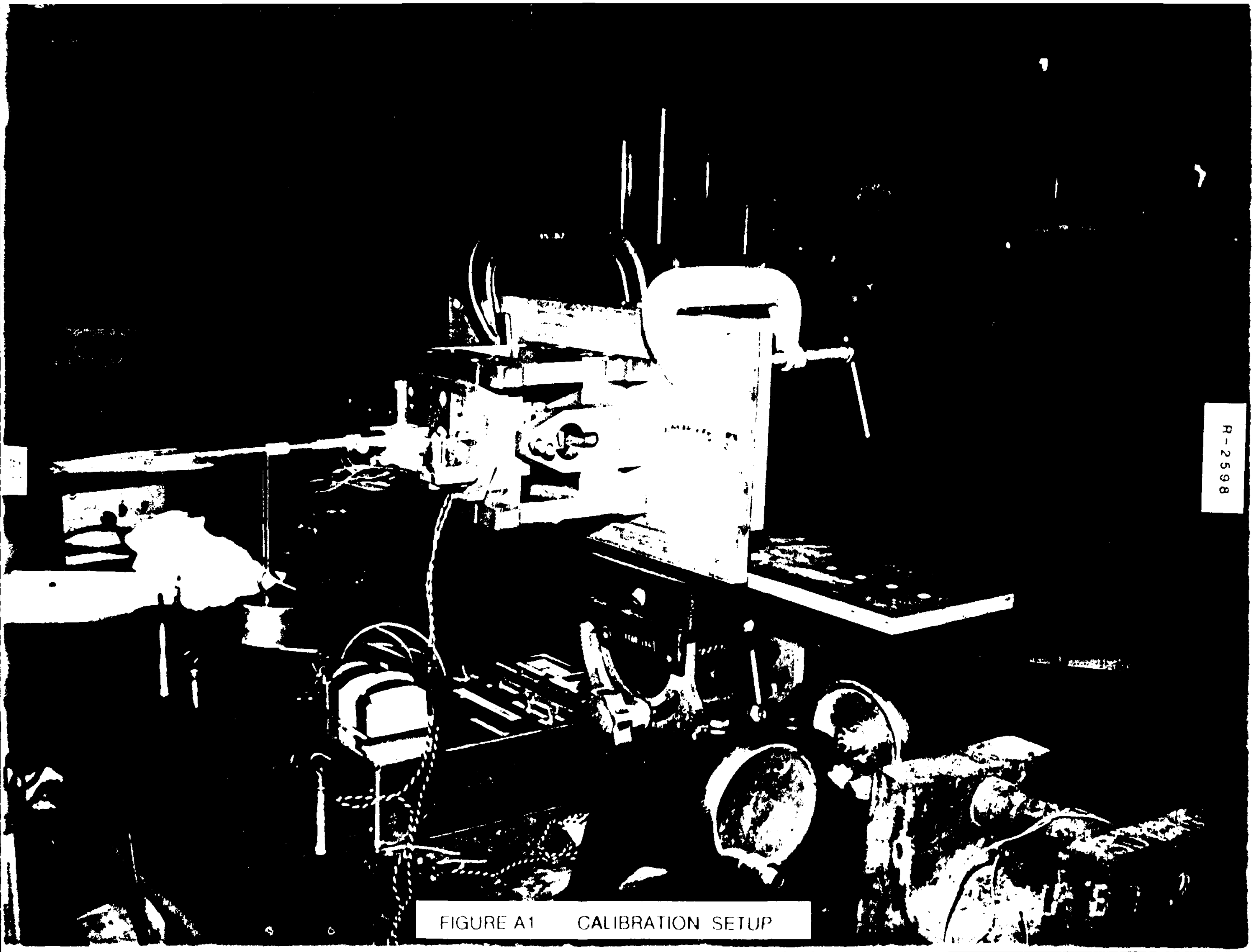

FIGURE A1 CALIBRATION SETUP

A5/A6

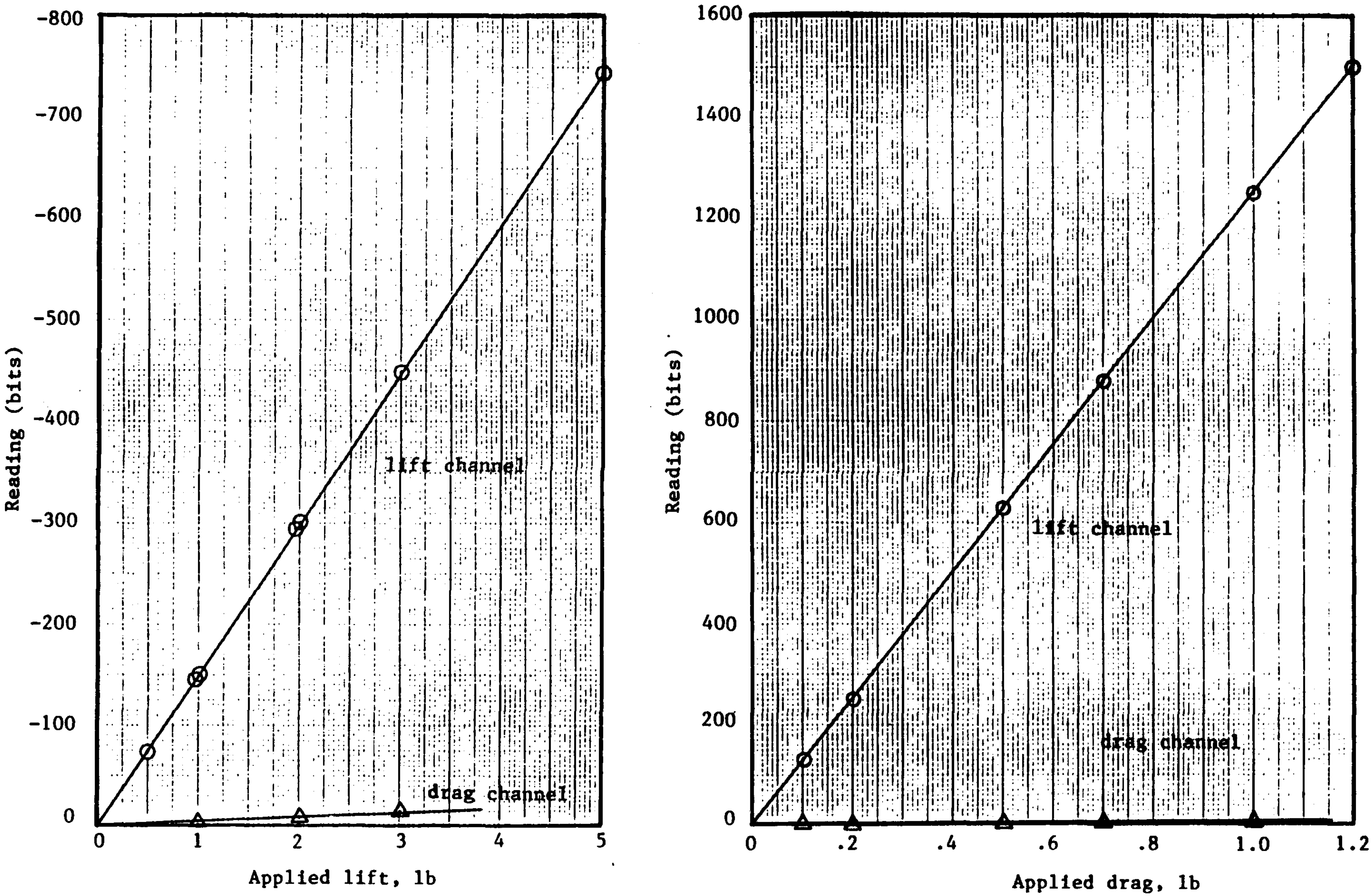

FIGURE A2 CALIBRATION OF LIFT AND DRAG BALANCE

APPENDIX B

TABULATION OF WATER TEMPERATURES

Date (1987)	Runs	Temperature (°F)
3/11	43-72	72.4
3/12	80-161	72.4
3/13	167-257	72.7
3/16	265-336	71.9
3/17	359-404	71.8
3/18	408-514	71.7
3/19	520-574	71.8
3/20	582-667	71.7
3/23	671-743	70.4
3/24	746-853	69.9
3/25	856-967	69.5
3/26	974-1019	69.2